(CNDO/2 calculations).[51] This effect will enhance the singlet–triplet separation since exchange through the π system by the DSP mechanism is inversely related to the energy difference between the π and π^* levels. Gerloch and Harding[53] also have reported semiempirical MO calculations in support of a π-type mechanism for superexchange.

de Loth et al.[50] have reported that higher order effects, SE, SE + P, contribute to the singlet–triplet splitting. The presence of an α-silicon atom in the ligand should enhance this effect by increasing the polarizability of the ligand. Kuznesof et al. have suggested that the greater stability of $H_3SiCO_2^-$, as compared to $H_3CCO_2^-$, is related to the greater polarizability of silicon.[51]

In conclusion, the large singlet–triplet splittings observed for copper(II) complexes of carboxysilanes and -germanes undoubtedly arise from the ability of the metalloid to interact with both the σ and π systems of the carboxylate group and to enhance the polarizability of the ligand.

Acknowledgment. We wish to thank Dr. D. W. Pratt, University of Pittsburgh, for the use of his ESR facilities, Drs. I. B. Goldberg and T. M. McKinney, Rockwell International, for running an ESR spectrum of the complex $Cu(O_2CSiPhMe_2)_2 \cdot H_2O$, and E. Horey, Carnegie-Mellon University, for his assistance with the magnetic susceptibility measurements by the Faraday method. The authors also wish to thank Dr. D. Finseth of the Pittsburgh Energy and Technology Center for the use of the Knauer VPO.

Registry No. $[Cu(O_2CCMe_2Ph) \cdot H_2O]_2$, 100229-28-5; $[Cu(O_2CSiMe_2Ph) \cdot H_2O]_2$, 100229-29-6; $[Cu(O_2CMePh_2) \cdot H_2O]_2$, 100229-30-9; $[Cu(O_2CSiMePh_2) \cdot H_2O]_2$, 100229-31-0; $[Cu(O_2CCPh_3) \cdot H_2O]_2$, 100229-32-1; $[Cu(O_2CSiPh_3) \cdot H_2O]_2$, 100243-55-8; $[Cu(O_2CGePh_3) \cdot H_2O]_2$, 100243-56-9; $[Cu(O_2CGePh_3) \cdot H_2O]_2$, 100243-57-0; $[Cu(O_2CGePh_3) \cdot H_2O]_2$, 100243-58-1; $[Cu(O_2CGePh_3) \cdot H_2O]_2$, 100243-59-2; $[Zn(O_2CSiMePh_2) \cdot 0.5H_2O]_2$, 100229-33-2.

Supplementary Material Available: Tables of analytical data, observed and calculated structure factors, thermal parameters, bond distances and angles, and intermolecular distances between **1** and **2** and a stereoscopic view of the unit cell of **1** (24 pages). Ordering information is given on any current masthead page.

---

(53) Gerloch, M.; Harding, J. H. *Proc. R. Soc. London, A* **1978**, *360*, 211.

Contribution from the Departments of Chemistry, McMaster University, Hamilton, Ontario, Canada L8S 4M1,
and University of Toronto, Toronto, Ontario, Canada M5S 1A1

Preparations, Raman Spectra, and Crystal Structures of $(SCl_3)(SbCl_6)$, $(SeCl_3)(SbCl_6)$, $(SBr_{1.2}Cl_{1.8})(SbCl_6)$, $(TeCl_3)(AlCl_4)$ (Triclinic Modification), $(TeCl_3)(SbF_6)$, $(TeCl_3)(AsF_6)$, and $(TeF_3)_2(SO_4)$

Beverley H. Christian, Michael J. Collins, Ronald J. Gillespie,* and Jeffery F. Sawyer*

Received April 26, 1985

The preparations, Raman spectra, and crystal structures of the compounds $(SCl_3)(SbCl_6)$ (**1**), $(SeCl_3)(SbCl_6)$ (**2**), $(SBr_{1.2}Cl_{1.8})(SbCl_6)$ (**3**), $(TeCl_3)(AlCl_4)$ (**4**), $(TeCl_3)(AsF_6)$ (**5**), $(TeCl_3)(SbF_6)$ (**6**), and $(TeF_3)_2SO_4$ (**7**) are reported. Crystal data are as follows: **1**, monoclinic, space group $C2/m$, $a = 12.385$ (2) Å, $b = 7.774$ (1) Å, $c = 13.959$ (3) Å, $\beta = 108.06$ (1)°, $V = 1277.8$ Å^3, and $D_c = 2.46$ g cm^{-3} for $Z = 4$; **2**, trigonal, space group $R\bar{3}m$, $a = 8.840$ (5) Å, $\alpha = 74.89$ (5)°, $V = 630.0$ Å^3, and $D_c = 2.74$ g cm^{-3} for $Z = 2$; **3**, trigonal, space group $R\bar{3}m$, $a = 8.871$ (2) Å, $\alpha = 74.11$ (2)°, $V = 630.7$ Å^3, and $D_c = 2.77$ g cm^{-3} for $Z = 2$; **4**, triclinic, space group $P\bar{1}$, $a = 6.554$ (1) Å, $b = 16.691$ (4) Å, $c = 8.391$ (1) Å, $\alpha = 92.79$ (1)°, $\beta = 97.31$ (1)°, $\gamma = 96.11$ (1)°, $V = 1065.8$ Å^3, and $D_c = 2.51$ for $Z = 4$; **5**, monoclinic, space group $P2_1/n$, $a = 8.827$ (2) Å, $b = 10.009$ (3) Å, $c = 10.592$ (5) Å, $\beta = 108.27$ (3)°, $V = 888.7$ Å^3, and $D_c = 3.26$ g cm^{-3} for $Z = 4$; **6**, orthorhombic, space group $Pnma$, $a = 17.031$ (3) Å, $b = 8.460$ (1) Å, $c = 6.398$ (1) Å, $V = 921.8$ Å^3, and $D_c = 3.38$ g cm^{-3} for $Z = 4$; **7**, orthorhombic, space group $P2_12_12_1$, $a = 8.758$ (1) Å, $b = 8.983$ (1) Å, $c = 9.946$ (2) Å, $V = 8.983$ Å^3, and $D_c = 3.95$ g cm^{-3} for $Z = 4$. Crystals of $(TeCl_3)(SbCl_6)$ and $(TeCl_3)(NbCl_6)$ are isomorphous, monoclinic, space group $C2/c$, with cell dimensions ($NbCl_6^-$ salt in brackets) $a = 22.137$ (4) Å [21.858 (4) Å], $b = 12.781$ (2) Å [12.622 (3) Å], $c = 19.308$ (3) Å [19.048 (3) Å], $\beta = 112.47$ (1)° [112.48 (1)°], $V = 5048$ (2) Å^3 [4856 (3) Å^3], and $D_c = 2.99$ g cm^{-3} [2.95 g cm^{-3}] for $Z = 16$. All the MX_3^+ cations in these compounds are involved in significant anion–cation secondary bonding interactions of varying strengths and geometries. Trans relationships between the lengths of these interactions and primary bond lengths and their effects on the primary bonding geometries of the cations are discussed and compared to those of related compounds. The $SBr_{1.2}Cl_{1.8}^+$ cation in the hexachloroantimonate salt consists of a disordered mixture of $SBr_xCl_{3-x}^+$ cations. The tetrachloroaluminate salt of $TeCl_3^+$ is a different modification with a crystal packing significantly different from that previously reported.

Introduction

An important feature of the crystal structures of salts containing MX_3^+ cations (M = S, Se, Te; X = F, Cl, Br, I) is the strong secondary interactions[1] between the cations and the accompanying anions. These interactions generally form around the lone pair of electrons on the central atom M in directions that are approximately capping faces (Y contacts) or bridging edges (Y′ contacts) of the polyhedron describing the primary geometry.[2] With the exception of $(TeF_3)(Sb_2F_{11})$, all reported structures containing MX_3^+ cations have three face-capping M···Y secondary interactions approximately trans to the primary bonds to give distorted monocapped octahedra AX_3Y_3E about M with the lone pair as the cap. In this paper we report the Raman spectra and crystal structures for the compounds $(SCl_3)(SbCl_6)$, $(SeCl_3)(SbCl_6)$, $(SCl_{1.2}Br_{1.8})(SbCl_6)$, $(TeCl_3)(AlCl_4)$, $(TeCl_3)(SbF_6)$, $(TeCl_3)(AsF_6)$, and $(TeF_3)_2(SO_4)$ and discuss trends in the overall MX_3^+ geometry and the strength of the anion–cation interactions with changing M and/or X in these and related salts. The tetrachloroaluminate salt of $TeCl_3^+$ is a different modification (triclinic) from that previously reported (monoclinic).[3]

Experimental Section

Materials. Sulfur (BDH, sublimed), selenium (Alfa Inorganics), and tellurium (Alfa Inorganics) were dried under vacuum at 20 °C. Arsenic (Alfa Inorganics) was heated under vacuum at 200 °C to sublime off the oxide. Bromine (Fisher Scientific Co.), methylene chloride (Fisher

---

*To whom correspondence should be addressed: R.J.G., McMaster University; J.F.S., University of Toronto.

(1) Alcock, N. W. *Adv. Inorg. Chem. Radiochem.* **1973**, *15*, 1.

(2) Sawyer, J. F.; Gillespie, R. J., submitted for publication in *Prog. Inorg. Chem.*

(3) Krebs, B.; Buss, B.; Altena, D. *Z. Anorg. Allg. Chem.* **1971**, *386*, 257.

0020-1669/86/1325-0777$01.50/0 © 1986 American Chemical Society

Scientific Co.), and sulfur dioxide (Canadian Liquid Air) were stored over P_4O_{10} before use. Antimony pentachloride (J. T. Baker, analyzed) was used as received. Aluminum trichloride (McArthur Chemical Co.) was twice vacuum sublimed through aluminum foil and pellets to remove $FeCl_3$. Arsenic pentafluoride was prepared from the elements. Crystalline S_7TeCl_2, prepared by following the method of Weiss and Pupp,[4] was characterized by X-ray methods (precession photographs).[5] Tellurium tetrafluoride was prepared by following the method of Lentz et al.[6] Antimony pentafluoride (Ozark-Mahoning) was purified by distillation under vacuum.

Preparation of $(SCl_3)(SbCl_6)$. Powdered, dried As_4S_4 (0.2719 g, 0.06353 mmol) was placed in one side of a double-arm vessel in a drybox and antimony pentachloride (~1.5 mL, ≥11.4 mmol) was syringed into the other. The arm containing the As_4S_4 was cooled in liquid nitrogen and the $SbCl_5$ poured through the frit separating the two arms. No reaction on contact of the $SbCl_5$ with the As_4S_4 at low temperature or room temperature was observed. After addition of SO_2, the mixture was heated. A deep red color formed, which quickly disappeared on stirring to give a pale yellow solution. After 24 h the SO_2 was pumped off and $SbCl_3$ and $(SCl_3)(SbCl_6)$ were separated by vacuum sublimation.

Preparation of $(SeCl_3)(SbCl_6)$. Dried powdered 1:1 As/Se melt (0.3637 g, 0.5909 mmol, assuming As_4Se_4) and antimony pentachloride (~1.4 mL, ≥10.6 mmol) were placed in a double-arm vessel in a drybox. The $SbCl_5$ was poured through the frit onto the As/Se powder cooled to −196 °C. On warming slightly, an exothermic reaction occurred, which raised the temperature to 60 °C, and the reaction mixture became blood red. Continued reaction rapidly gave a light green-yellow solution. After 24 h SO_2 was added to dissolve the $SbCl_3$, leaving insoluble $(SeCl_3)(SbCl_6)$.

Preparation of $(SeCl_3)(SbCl_6)$ from $SeCl_4$ and $SbCl_5$. Crystals of $SeCl_4$ (0.1093 g, 0.4951 mmol) were placed into a double-arm vessel in the drybox. Antimony pentachloride (0.1 mL, ≥ 0.50 mmol) was syringed onto the $SeCl_4$. No reaction was apparent over the next hour. Sulfur dioxide was then distilled into the vessel and stirred overnight. The SO_2 was then slowly distilled off, leaving $(SeCl_3)(SbCl_6)$ and some unreacted $SbCl_5$, which could be dissolved in a small amount of SO_2.

Preparation of $(SBr_{1.2}Cl_{1.8})(SbCl_6)$—Attempted Preparation of $(SBr_3)(SbCl_6)$. Dry sulfur (0.2056 g, 6.412 mmol) and ca. 0.80 mL (6.4 mmol) of $SbCl_5$ were placed into the arms of a double-arm vessel in a drybox. Bromine (12.83 mmol) was distilled onto the sulfur at −196 °C. When the vessel was allowed to warm to room temperature, the bromine reacted with the sulfur. The $SbCl_5$ was then poured through the frit onto the mixture, resulting in a reddish solution. After the mixture was stirred overnight, excess $SbCl_5$, Br_2, and $SbCl_3$ were removed by washing with small portions of SO_2, leaving yellow translucent crystals of $(SBr_{1.2}Cl_{1.8})(SbCl_6)$.

Preparation of $(TeCl_3)(SbCl_6)$. Tellurium (0.4016 g, 3.147 mmol) and an excess of $SbCl_5$ (4.67 g, 15.6 mmol) were added to separate sides of a double-bulb vessel in a drybox. Thirty milliliters of SO_2 was condensed onto the $SbCl_5$ and the yellow solution poured onto the Te with stirring. A pale magenta solution color typical of Te_4^{2+} was observed.[7] After 2 h all the Te had reacted, producing a yellow solution free of residue. The vessel was heated at 65 °C for 24 h with no apparent change. After some of the solvent was slowly distilled to the other bulb, large yellow crystals were deposited. The Raman spectrum of these crystals indicated that they were $(TeCl_3)(SbCl_6)$.

Preparation of $(TeCl_3)(AlCl_4)$. Thirty milliliters of CH_2Cl_2 was distilled onto a mixture of $AlCl_3$ (0.533 g, 4.00 mmol) and S_7TeCl_2 (0.846 g, 2.00 mmol) in a double-bulb vessel. The resulting solution had the characteristic orange color of S_7TeCl_2, but after the mixture was stirred for 24 h, the color changed to a bright yellow and a large quantity of white powder precipitated. The powder was filtered off and recrystallized from CH_2Cl_2, producing thin white plates, which were identified by Raman spectroscopy and X-ray crystallography as a new form of $(TeCl_3)(AlCl_4)$. Yellow, block-like crystals, which also formed from the original reaction mixture, were identified as S_8 (orthorhombic, *Fddd*) from precession photographs.[8]

Preparation of $(TeCl_3)(AsF_6)$. Arsenic pentafluoride (0.226 g, 1.33 mmol) and SO_2 (20 mL) were distilled onto $TeCl_4$ (0.2383 g, 0.8845 mmol) in a double-bulb vessel. After 24 h of stirring the solution was a pale yellow color. Stirring for 1 week produced no further change. A large quantity of white powder, which formed upon slow removal of the solvent, was transferred to another vessel and recrystallized as thin colorless plates from a 1:4 CH_2Cl_2/SO_2 mixed solvent. X-ray crystallography identified these crystals as $(TeCl_3)(AsF_6)$.

Preparation of $(TeCl_3)(SbF_6)$—Attempted Recrystallization of $TeF_4{\cdot}SbF_5$. Tellurium tetrafluoride (0.4714 g, 2.315 mmol) was combined with SbF_5 (0.4970 g, 2.293 mmol) and 30 mL of SO_2 in a double-bulb vessel, and the reaction mixture was stirred for 2 h before the SO_2 was slowly distilled off of the colorless solution, leaving a white powder. This product, presumably $TeF_4{\cdot}SbF_5$,[9,10] was too soluble in SO_2 to obtain good crystals so a portion of the product (0.4842 g, 1.152 mmol $TeF_4{\cdot}SbF_5$) was transferred into another double-bulb vessel, along with 15 mL of SO_2 and 20 mL of CH_2Cl_2, producing a colorless solution free of residue. A large quantity of white powder precipitated after half of the solvent had been slowly removed by distillation. The remaining solvent, presumably mostly composed of the less volatile CH_2Cl_2, was left over the powder to encourage crystal growth. After 2 weeks the solution was a pale pink color, and thin, colorless plate- and needle-shaped crystals of $(TeCl_3)(SbF_6)$ had formed at the vapor–liquid interface.

Preparation of $(TeF_3)_2(SO_4)$. Thirty milliliters of SO_2, 2.198 g of AsF_5 (12.87 mmol) and a trace of Br_2 (20 mg) were condensed onto a mixture of Te (0.8115 g, 6.360 mmol) and Se (0.5082 g, 6.436 mmol) in a double-bulb vessel. The reaction mixture was stirred, producing green and then brown and blood-red solutions, returning to green after 2 h of mixing. These colors are consistent with the initial formation in solution of Se_8^{2+} and/or Se_{10}^{2+} (both green)[11] followed by the production of mixed Te–Se cations (red or brown),[12] which react further to produce colorless TeF_3^+ and more Se_8^{2+} and/or Se_{10}^{2+}. After 24 h a large quantity of finely divided black powder had precipitated. The green solution was filtered and the solvent slowly distilled off, leaving a deep green oil. A few milliliters of SO_2 were distilled onto this oil in an NMR tube, and the ^{77}Se NMR spectrum of this solution identified the Se_{10}^{2+} cation.[13] No other species were observed. After several weeks a few colorless crystals that formed in the NMR tube were shown to be $(TeF_3)_2(SO_4)$ by X-ray crystallography.

Spectra. Raman spectra were obtained on the instrument previously described.[14] The samples were in the preparation vessel or were sealed in $^1/_4$ in o.d. Pyrex tubes.

X-ray Crystallography. All crystals were sealed in Lindemann capillaries in a drybox equipped with a microscope. Precession photographs were used to check crystal quality and to obtain preliminary cell and symmetry information. Crystal data for each compound are summarized in Table I. Details of the intensity measurements and structure refinements are given in Table II. With the exception of $(SeCl_3)(SbCl_6)$, no systematic trends in the intensities of the standard reflections for each data set were observed. Lorentz and polarization corrections were applied to all the data. Absorption corrections, if applied, were made by using the program ABSORB of the Enraf-Nonius SDP or XRAY systems.[15,16] Averaging of equivalent data and the exclusion of systematically absent and weak or zero F_o data gave the final totals of independent reflections shown in Table II.

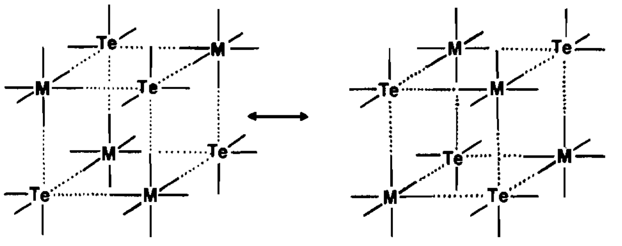

I II

M = Sb, Nb

---

(4) Weiss, J.; Pupp, M. *Angew. Chem., Int. Ed. Engl.* **1971**, *9*, 463.

(5) Weiss, J.; Pupp, M. *Acta Crystallogr., Sect. B: Struct. Crystallogr. Cryst. Chem.* **1972**, *B28*, 3653.

(6) Lentz, D.; Pritzkow, H.; Seppelt, K. *Inorg. Chem.* **1978**, *17*, 1926.

(7) Burns, R. C.; Gillespie, R. J.; Luk, W.-C.; Slim, D. R. *Inorg. Chem.* **1979**, *18*, 3086.

(8) Abrahams, S. C. *Acta Crystallogr.* **1955**, *8*, 661.

(9) Bartlett, N.; Robinson, P. L. *J. Chem. Soc.* **1961**, 3417.

(10) Evans, J. A.; Long, D. A. *J. Chem. Soc. A* **1968**, 1688.

(11) Burns, R. C.; Chan, W.-L.; Gillespie, R. J.; Luk. W.-C.; Sawyer, J. F.; Slim, D. R. *Inorg. Chem.* **1980**, *19*, 1432.

(12) Gillespie, R. J.; Luk, W.-C.; Maharajh, E.; Slim, D. R. *Inorg. Chem.* 1977, *16*, 892. Boldrini, P.; Brown, I. D.; Collins, M. J.; Gillespie, R. J.; Maharajh, E.; Sawyer, J. F.; Slim, D. R. *Inorg. Chem.* **1985**, *24*, 4302.

(13) Burns, R. C.; Collins, M. J.; Gillespie, R. J.; Schrobilgen, G. J., unpublished data.

(14) Burns, R. C.; Gillespie, R. J.; Luk, W.-C. *Inorg. Chem.* **1978**, *17*, 3596.

(15) "Enraf-Nonius Structure Determination Package"; B. A. Frenz and Associates, Inc.: College Station, TX, 1981.

(16) "XRAY71 and XRAY 76 Systems of Crystallographic Programs"; Technical Reports TR-102 and TR-446; University of Maryland Computer Center: College Park, MD, 1971 and 1976.

Table I. Crystal Data

compd	cryst syst	a, Å	b, Å	c, Å	α, deg	β, deg	γ, deg	V, Å^3	fw	Z	D_{calcd}, g/cm^3	space group	μ- (Mo K$\bar{\alpha}$), cm^{-1}	no. of reflcns used in cell determn (2θ range, deg)
$(TeF_3)_2(SO_4)$	ortho-rhombic	8.758 (1)	8.983 (1)	9.946 (2)	90	90	90	782.5 (3)	465.3	4	3.95	$P2_12_12_1$	78.3	25 ($13 < 2\theta < 32$)
$(TeCl_3)(SbF_6)$	ortho-rhombic	17.031 (3)	8.460 (1)	6.398 (1)	90	90	90	921.8	469.7	4	3.38	$Pnma$	70.4	25 ($10 < 2\theta < 40$)
$(TeCl_3)(AsF_6)$	monoclinic	8.827 (2)	10.009 (3)	10.592 (5)	90	108.27 (3)	90	888.7	422.9	4	3.26	$P2_1/n$	79.9	25 ($23 < 2\theta < 34$)
$(TeCl_3)(AlCl_4)$	triclinic	6.554 (1)	16.691 (4)	8.391 (1)	92.79 (1)	97.31 (1)	96.11 (1)	1065.8 (3)	402.7	4	2.51	$P\bar{1}$	46.3	15 ($27 < 2\theta < 30$)
$(TeCl_3)(AlCl_4)^a$	monoclinic	6.600 (5)	12.675 (8)	13.678 (8)	90	105.72 (5)	90	1093 (3)	402.7	4	2.51	$C2/c$	46.3	
$(TeCl_3)(SbCl_6)$	monoclinic	22.137 (4)	12.781 (2)	19.308 (3)	90	112.47 (1)	90	5048 (2)	568.8	16	2.99	$C2/c$ or Cc^c	63.9	15 ($30 < 2\theta < 34$)
$(TeCl_3)(NbCl_6)^b$	monoclinic	21.858 (4)	12.622 (3)	19.048 (3)	90	112.48 (1)	90	4856 (3)	539.6	16	2.95	$C2/c$ or Cc^c	52.6	25 ($13 < 2\theta < 30$)
$(SCl_3)(SbCl_6)$	monoclinic	12.385 (2)	7.774 (1)	13.959 (3)	90	108.06 (1)	90	1277.8 (4)	472.8	4	2.46	$C2/m$	42.6	15 ($29 < 2\theta < 32$)
$(SBr_{1.2}Cl_{1.8})$-$(SbCl_6)$	trigonal	10.691 (1)	10.691 (2)	19.113 (4)	90	90	120	1892.1 (7)	526.2	6	2.77	$R\bar{3}m$	79.7	15 ($30 < 2\theta < 35$)
		8.871 (2)	8.871 (2)	8.871 (2)	74.11 (2)	74.11 (2)	74.11 (2)	630.7 (2)		2				
$(SeCl_3)(SbCl_6)$	trigonal	10.750 (8)	10.750 (8)	18.885 (8)	90	90	120	1890 (2)	519.7	6	2.74	$R\bar{3}m$	71.5	15 ($20 < 2\theta < 35$)
		8.840 (5)	8.840 (5)	8.840 (5)	74.89 (5)	74.89 (5)	74.89 (5)	630.0 (6)		2				

[a] Reference 3. [b] Data collected on the related $I2/a$ cell with a = 19.048 (3) Å, b = 12.622 (3) Å, c = 22.852 (3)Å, and β = 117.89 (1)°. [c] The structures of I and II in the centric space group $C2/c$ consist of a disordered mixture of the cubane arrangements (Sawyer, J. F., unpublished data).

Structure Solutions. Although both $(TeCl_3)(AlCl_4)$ and $(TeF_3)_2(SO_4)$ were initially of unknown composition, a combination of Patterson and direct methods gave several atomic positions in each case. Other structures were solved by the use of the Patterson function to locate the heavy atoms after suitable consideration of any space group alternatives.[17] Subsequent cycles of least-squares and Fourier calculations then located all the remaining atoms. Absorption corrections were applied when necessary, and suitable weighting schemes were introduced. Least-squares refinement of each structure then converged to give the residuals in Table II.

For all structures neutral-atom scattering curves were taken from ref 18. Computing was performed on CDC 6400, CYBER 72, and PDP 11/23 computers using programs in the XRAY,[16] SHELX[19] and Enraf-Nonius SDP systems.[15] The final atomic parameters for all structures are given in Table III.

Discussion of Crystal Structures

1. $(SCl_3^+)(SbCl_6^-)$. The SCl_3^+ cation has crystallographic mirror symmetry and a tetrahedral AX_3E primary bond geometry.[20] The dimensions of the present SCl_3^+ cation are slightly different from those of the cations in $(SCl_3^+)(ICl_4^-)$,[21a] $(SCl_3^+)(AlCl_4^-)$,[21b] $(SCl_3^+)(UCl_6^-)$,[21c] and, most recently, $(SCl_3^+)(AsF_6^-)$[21d] due to anion–cation interactions (Table IV). Thus, there is a significant decrease in the S–Cl bond length in going from the ICl_4^- salt (1.992 (3) Å av) to the $SbCl_6^-$ and UCl_6^- salts (1.956 (3) and 1.962 (14) Å av, respectively) with a corresponding lengthening of the secondary S···Cl contacts from 3.115 (3) Å (av) in the ICl_4^- salt to 3.220 (4) Å (av) and 3.238 Å (av) in the $SbCl_6^-$ and UCl_6^- salts. The primary bond lengths and secondary contact distances in the $(SCl_3)(AlCl_4)$ salt are, however, intermediate between those in $(SCl_3)(ICl_4)$ and those in $(SCl_3)(SbCl_6)$. The weakest secondary contacts are the S···F contacts in $(SCl_3)(AsF_6)$ (av 2.90 Å), and this SCl_3^+ cation has the shortest S–Cl bond lengths. This is as expected if chlorine (and fluorine) atoms in the anions donate electron density into antibonding σ^* orbitals associated with the S–Cl σ bonds of the cation.[1] Correlations between these primary and secondary bond distances and the S–Cl stretching frequencies are discussed in ref 21d.

The additional contacts in each salt give an overall distorted monocapped octahedral AX_3Y_3E geometry around each sulfur atom with trans X–A–Y angles in the range 152.7–167.2 (1)° (Table IV). Consistent with the weaker nature of the secondary contacts and the stronger primary S–Cl bonds, there is also an increase in the primary Cl–S–Cl angle in the $SbCl_6^-$ salt (102.2 (1) and 104.4 (1)° (×2)) (and $(SCl_3^+)(UCl_6^-)$) over that in the

---

(17) For $(SCl_{1.2}Br_{1.8})(SbCl_6)$ and $(SeCl_3)(SbCl_6)$ the absence of any systematic absences was consistent with the trigonal space groups $R3$, $R3m$, $R\bar{3}$, $R32$, and $R\bar{3}m$. The value of $Z = 2$ indicates that the Sb and S(Se) atoms must be on special positions, so symmetry arguments were used to rule out $R3$ and $R3m$. The subsequent interpretation of the Patterson fuction then concentrated on a the centric space groups $R\bar{3}$ and $R\bar{3}m$, and a reasonable solution for $(SCl_{1.2}Br_{1.8})(SbCl_6)$ was obtained in $R\bar{3}m$ by placing the Sb atoms on the special positions 1(a) and 1(b) with $\bar{3}m$ symmetry and an atom, which was initially assumed to be bromine, on the special position 6(h). Subsequent difference maps then gave the positions of the chlorines bonded to the antimony atoms (6(g) and 6(f)) and two sulfur positions (2(c)) with symmetry $3m$. Least-squares refinement indicated a high temperature factor for the bromine, which, along with the different sulfur positions, suggested that this atom was disordered. This was confirmed when the overall site occupancy for this position (as well as those for the two alternative sulfur sites) were allowed to vary. In the refinement of $(SeCl_3)(SbCl_6)$ the coordinates from $(SCl_{1.2}Br_{1.8})(SbCl_6)$ were used with the scattering curves for Se and Cl replacing those of S and Br.

(18) "International Tables for X-Ray Crystallography"; Kynoch Press: Birmingham, England, 1965.

(19) Sheldrick, G. M. "SHELX—Program for Crystal Structure Determination", University of of Cambridge, 1976.

(20) Gillespie, R. J. "Molecular Geometry"; Van Nostrand Reinhold: London, 1972.

(21) (a) Edwards, A. J. *J. Chem. Soc., Dalton Trans.* **1978**, 1723. (b) Trojanow, S. I.; Kolditz, L.; Radde, A. *Z. Chem.* **1983**, *23*, 136. (c) Sawodny, W.; Rediess, K.; Thewalt, U. *Z. Anorg. Allg. Chem.* **1983**, *499*, 81. (d) Minkwitz, R.; Janichen, K.; Prenzel, H.; Wolfel, V. *Z. Naturforsch, B: Anorg. Chem., Org. Chem.* **1985**, *40B*, 53. This paper also includes brief data for a second determination of $(SCl_3)(SbCl_6)$ with a slightly longer average S–Cl distance of 1.974 Å (no standard deviations given) (Krebs, B.; Gretenkord, K. and Luhrs, E. *Z. Anorg. Allg. Chem.*, in press).

Table II. Details of Intensity Measurements and Structure Refinements

	$(TeF_3)_2(SO_4)$	$(TeCl_3)(SbF_6)$	$(TeCl_3)(AsF_6)$	$(TeCl_3)(AlCl_4)$ (triclinic)	$(SCl_3)(SbCl_6)$	$(SeCl_3)(SbCl_6)$	$(SCl_{1.2}Br_{1.8})(SbCl_6)$
				Data Collections			
diffractometer	CAD4	CAD4	CAD4	Syntex	Syntex	Syntex	Syntex
mode	$\theta-2\theta$	$\theta-2\theta$	$\theta-2\theta$	$\theta-2\theta$	$\theta-2\theta$	$\theta-2\theta$	$\theta-2\theta$
radiation[k]	Mo $K\bar{\alpha}$	Mo $K\bar{\alpha}$	Mo $K\bar{\alpha}$	Mo $K\bar{\alpha}$	Mo $K\bar{\alpha}$	Mo $K\bar{\alpha}$	Mo $K\bar{\alpha}$
scan range, deg	$K\alpha_1 - 1.5$ to $K\alpha_2 + 1.5$	$K\alpha_1 - 0.90$ to $K\alpha_2 + 0.90$	$K\alpha_1 - 0.85$ to $K\alpha_2 + 0.85$	$K\alpha_1 - 0.90$ to $K\alpha_2 + 0.90$	$K\alpha_1 - 0.85$ to $K\alpha_2 + 0.85$	$K\alpha_1 - 1.2$ to $K\alpha_2 + 1.2$	$K\alpha_1 - 1.0$ to $K\alpha_2 + 1.0$
scan speeds, deg/min	2.0–10.0	1.0–6.7	1.0–10.0	3.0–29.3	2.0–29.3	4.5–29.3	2.0–29.3
max 2θ, deg	55	55	55	50	55	50	60
bkgd	*l*	*l*	*l*	*l*	*l*	*l*	*l*
no. of std. reflcns/interval, s or reflcns	1/800	3/10 000	3/8000	3/67	3/67	2/48	3/37
				Details of Refinements			
abs cor					none	none	none
cryst faces: *d*, cm	{0,0,1}: 0.0125 {1,1,0}: 0.0047	{0,1,0}: 0.0080 {0,0,1}: 0.0056 {1,0,0}: 0.0022	$(1,0,\bar{1})$: 0.0022 $(\bar{1},0,1)$: 0.0022 $(\bar{1},0,\bar{2})$: 0.0075 (0,2,1): 0.0063 $(0,\bar{2},1)$: 0.0088	{0,0,1}: 0.0087 {0,1,0}: 0.0075 (2,1,0): 0.0140 $(2,\bar{1},0)$: 0.0140 $(\bar{2},\pm1,1)$: 0.0036 $(\bar{2},\pm1,\bar{1})$: 0.0036			
cryst shape; dimens, cm					block; 0.02 × 0.025 × 0.025	plate; 0.025 × 0.025 × 0.005	needle; 0.02 × 0.02 × 0.045
grid	8 × 8 × 12	8 × 6 × 12	8 × 10 × 8	6 × 10 × 9			
range transmission	0.451–0.518	0.460–0.736	0.372–0.848	0.515–0.573			
no. of nonzero data[a]	2049[b]	2019[c]	2367[d]	4319[e]	2313[f]	1481[g]	3004[h]
no. of data with $F \geq 6.0\sigma(F)$	1573	781	1892	2876	1400[i]	248	520
R_1	0.053	0.029	0.038	0.030	0.038	0.062	0.031
R_2	0.054	0.030	0.047	0.037	0.044	0.062	0.031
max shift/error	0.08	0.32	0.03	0.07	0.09	0.18	0.07
weighting scheme[j]	A	B	B	A	A	A	A
m	1.0			4.0	1.7	1.0	1.0
p	0.0066	0.050	0.055	0.0018	0.0007	0.0028	0.000 14
final ΔF Fourier max peak, e Å^{-3}	4.0 (near Te)	1.14 (near Sb)	0.79 (near Te)	1.5 (near Te)	3.2 (near Sb)	1.06 (near Cl)	0.75 (near Sb)

[a] Includes repeat measurements of standards ($T = 298$ K for all collections). [b] Quadrants $h,k,\pm l$. [c] Quadrants $h,\pm k,l$. [d] Quadrants $h,k,\pm l$. [e] Quadrants $h,\pm k,\pm l$. [f] Total includes all reflections in the quadrants $h,k,\pm l$ and several reflections in the quadrants $h,-k,\pm l$ with $2\theta \leq 35°$. Total number of data after averaging equivalent reflections is 1493. [g] Data collected on hexagonal cell (includes systematically absent reflections (*hkl*) with $h - k + l = 3n$, using the option that $h \geq k$ for reflections in the quadrants $h,k,\pm l$. [h] Data collected on rhombohedral cell. Crystal was recentered several times during data collection due to crystal movement as well as crystal decomposition (762 reflections recollected). All reflections (2317) in the quadrant h,k,l with $2\theta \leq 60°$ and a further 687 reflections with negative *l* indices were eventually collected. After rejection of the 762 intensities that were recollected, the data were rescaled for the slight crystal decomposition on the basis of the standard reflections. [i] $F > 2\sigma(F)$. [j] Scheme A: $w^{-1} = m\sigma(F)^2 + pF^2$(SHELX). Scheme B: $w = 4F^2[\sigma(I)^2 + (pF^2)^2]^{-1}$ (SDP). The suitability of these schemes were indicated by the absence of any local dependence of the average $w\|F_o| - |F_c\|^2$ as a function of F_o and sin θ. No extinction corrections were considered necessary. [k] $\lambda = 0.710\,69$ Å. [l] Stationary crystal–stationary counter at each end of scan.

ICl_4^- salt (100.7 (1)° and 101.9 (1)°). We conclude that, with respect to the SCl_3^+ cation, the anion $SbCl_6^-$ is a weaker Lewis base than ICl_4^-.

The $SbCl_6^-$ anion in the structure has crystallographic $2/m$ symmetry and approximate octahedral geometry. The chlorine atoms Cl(4) and Cl(6), which form the shorter contacts to sulfur, also form the longest Sb–Cl bonds (2.361 (2) Å (av) compared with 2.350 (2) Å for the noninteracting atoms). Similar distortions of the ICl_4^- anion in $(SCl_3^+)(ICl_4^-)$ have significant effects on the vibrational and ^{35}Cl NQR spectral data for this and related compounds.[22,23] The crystal packing in $(SCl_3^+)(SbCl_6^-)$ consists of layers of interacting anions and cations almost parallel to the *bc* plane.

2. $(SBr_{1.2}Cl_{1.8}^+)(SbCl_6^-)$. The cation in this compound has an average composition of $SBr_{1.2}Cl_{1.8}^+$ and is disordered over two sulfur sites with symmetry $\bar{3}m$. The population parameters of the two sulfur atoms (0.732 (1) and 0.270 (2)) and of the mixed Cl/Br site (refined as bromine with a population parameter of 0.690 (1)) indicate that the disorder might be described in terms of an "up" orientation of the SBr_3^+ cation and a "down" orientation of a SCl_3^+ cation. However, the Raman spectrum gives some evidence for other mixed $SBr_xCl_{3-x}^+$ ($x = 1, 2$) cations (see below). The S–X distances to the two sulfur sites are 2.076 Å (×3) and 2.039 (3) Å (×3) (Table V). The longer distance is significantly shorter than the S–Br distance in S_7Br^+ (2.18 (3) Å)[24] and the sum of the covalent radii of S and Br.[25] A bond length of 2.164 Å and bond angle of 101 (1)° have been predicted for SBr_3^+ on the basis of an analysis of other MX_3^+ (M = S, Se, Te; X = F, Cl, Br, I) and group V (Group 15[47]) trihalide species.[26] Similarly, the distance of 2.039 Å is significantly longer than the S–Cl distances in the SCl_3^+ cation above. Bond angles at the two sulfur sites are 105.3° (×3) and 108.1° (×3) with the smaller angle at the site with the longer S–X distances.

Secondary contacts complete the AX_3Y_3E monocapped octahedral coordination sphere of each sulfur atom. At S(1), the three S···Cl(2) contacts are of length 3.313 Å with *trans*-"Br"–S(1)···Cl(2) angles of 149.1° while at S(2) the three S···Cl(1)′ contacts are of length 3.232 Å with "Br"–S(2)···Cl(1) angles of 147.6°. The S···Cl secondary bonds to S(2) are comparable in length to the S···Cl distances in $(SCl_3)(SbCl_6)$ above; those to S(1) are somewhat longer.

---

(22) Finch, A.; Gates, P. N.; Page, T. H.; Dillon, K. B.; Waddington, T. C. *J. Chem. Soc., Dalton Trans.* **1980**, 2401.

(23) Finch, A.; Gates, P. N.; Page, T. H.; Dillon, K. B. *J. Chem. Soc., Dalton Trans.* **1983**, 1837.

(24) Passmore, J.; Sutherland, G.; White, P. S. *J. Chem. Soc., Chem. Commun.* **1980**, 330.

(25) Cotton, F. A.; Wilkinson, G. "Advanced Inorganic Chemistry", 4th ed.; Wiley-Interscience: Toronto, 1980.

(26) Passmore, J.; Richardson, E. K.; Whidden, T. K.; White, P. S. *Can. J. Chem.* **1980**, *58*, 851.

Table III. Final Atomic Positional Parameters ($\times 10^4$)

atom	*x*	*y*	*z*	K^a
(a) $(SCl_3^+)(SbCl_6^-)$				
Sb(1)	0	0	0	
Sb(2)	0	5000	5000	
S	8448 (1)	0	2799 (1)	
Cl(1)	7908 (2)	0	3976 (2)	
Cl(2)	7682 (2)	1955 (2)	1999 (1)	
Cl(3)	0	2975 (3)	0	
Cl(4)	389 (2)	0	1768 (2)	
Cl(5)	1975 (2)	0	274 (2)	
Cl(6)	332 (1)	2848 (2)	3929 (1)	
Cl(7)	3050 (1)	0	4101 (1)	
(b) $(SBr_{1.2}Cl_{1.8}^+)(SbCl_6^-)$ and $(SeCl_3^+)(SbCl_6^-)^b$				
Sb(1)	0	*x*	*x*	0.0833
Sb(2)	5000	*x*	*x*	0.0833
Br	3480 (1)	*x*	390 (1)	0.345 (2)
[Cl	3499 (6)	*x*	463 (8)	0.500]
Cl(1)	329 (1)	*x*	−2811 (2)	0.500
[	307 (5)	*x*	−2800 (7)	]
Cl(2)	3240 (1)	*x*	378 (2)	0.500
[	3229 (4)	*x*	361 (8)	]
S(1)	2880 (2)	*x*	*x*	0.122 (2)
[Se(1)	2966 (4)	*x*	*x*	0.077 (2)]
S(2)	2071 (5)	*x*	*x*	0.045 (2)
[Se(2)	2025 (5)	*x*	*x*	0.085 (3)]
(c) $(TeCl_3^+)(AlCl_4^-)$				
Te(1)	2473.6 (5)	6186.3 (2)	2607.4 (4)	
Te(2)	7183.6 (5)	1075.4 (2)	2871.0 (4)	
Al(1)	3146 (3)	3972 (1)	1185 (2)	
Al(2)	2778 (3)	1242 (1)	6727 (2)	
Cl(11)	1016 (3)	6015 (1)	4901 (2)	
Cl(12)	5668 (3)	6595 (1)	3913 (2)	
Cl(13)	1385 (3)	7238 (1)	2291 (2)	
Cl(14)	3727 (3)	4760 (1)	3095 (2)	
Cl(15)	1260 (3)	3141 (1)	1884 (2)	
Cl(16)	6053 (2)	3661 (1)	720 (2)	
Cl(17)	1802 (3)	4425 (1)	9077 (2)	
Cl(21)	4049 (3)	579 (1)	1630 (2)	
Cl(22)	6317 (3)	2162 (1)	2971 (2)	
Cl(23)	8692 (3)	1179 (1)	585 (2)	
Cl(24)	1343 (2)	1698 (1)	4662 (2)	
Cl(25)	5703 (3)	956 (1)	6178 (2)	
Cl(26)	901 (3)	325 (1)	7166 (2)	
Cl(27)	3174 (3)	1929 (1)	8724 (2)	
(d) $(TeCl_3^+)(SbF_6^-)$				
Sb(1)	4242.5 (5)	2500	8497 (1)	
Te(1)	1049.8 (4)	2500	1295 (1)	
Cl(1)	3562 (2)	−575 (3)	4075 (4)	
Cl(2)	7120 (2)	2500	1648 (7)	
F(1)	4715 (4)	2500	5840 (10)	
F(2)	3260 (4)	2500	7320 (20)	
F(3)	5245 (5)	2500	9610 (10)	
F(4)	3823 (8)	2500	11170 (10)	
F(5)	4268 (3)	297 (5)	8416 (8)	
(e) $(TeCl_3^+)(AsF_6^-)$				
Te(1)	659.5 (5)	1440.9 (4)	3194.4 (4)	
As	6091.6 (9)	2908.7 (7)	2246.6 (7)	
Cl(1)	1140 (3)	3635 (2)	3638 (2)	
Cl(2)	906 (3)	1520 (2)	1130 (2)	
Cl(3)	3182 (2)	723 (2)	4226 (2)	
F(1)	5432 (6)	3678 (5)	711 (5)	
F(2)	7725 (5)	2329 (5)	1839 (5)	
F(3)	5061 (7)	1551 (5)	1586 (7)	
F(4)	4463 (6)	3586 (6)	2568 (6)	
F(5)	6770 (9)	2152 (7)	3745 (6)	
F(6)	7086 (7)	4323 (6)	2860 (7)	
(f) $(TeF_3)_2SO_4$				
Te(1)	407.8 (9)	1427.2 (9)	411.8 (8)	
Te(2)	538.6 (10)	6654.4 (9)	−844.1 (8)	
S(1)	1700 (3)	4503 (4)	2073 (3)	
F(11)	2240 (9)	2090 (10)	−320 (10)	
F(12)	735 (12)	−408 (10)	−493 (10)	
F(13)	1559 (9)	649 (11)	1786 (9)	
F(21)	−841 (10)	7188 (11)	−2167 (8)	
F(22)	−1094 (11)	6867 (11)	332 (10)	
F(23)	3 (9)	4686 (9)	−1084 (9)	
O(1)	514 (10)	3406 (11)	1734 (9)	
O(2)	3224 (11)	3798 (14)	2072 (10)	
O(3)	1419 (12)	5052 (13)	3442 (10)	
O(4)	1709 (15)	5699 (13)	1090 (11)	

[a] Site occupancy factor *K* = site multiplicity × population parameter of the atom at each site. [b] Different values in square brackets correspond to the isomorphous $(SeCl_3^+)(SbCl_6^-)$ structure.

Table IV. Bond Lengths (Å) and Bond Angles (deg) for $(SCl_3^+)(SbCl_6^-)$, $(SCl_3^+)(ICl_4^-)$,[a] $(SCl_3^+)(UCl_6^-)$,[b] $(SCl_3^+)(AlCl_4^-)$,[c] and $(SCl_3^+)(AsF_6^-)$[d]

	$SbCl_6^-$ salt[e]	ICl_4^- salt	$AlCl_4^-$ salt	UCl_6^- salt
		Bond Lengths		
S(1)–Cl(1)	1.956 (3)	2.002 (3)	1.988 (9)	1.955 (14)
S(1)–Cl(2)	1.948 (2)	1.981 (2) (av)	1.955 (9), 1.978 (9)	1.973 (13), 1.959 (12)
S(1)–Cl(4)	3.162 (3)	3.097 (3)	3.268 (9)	3.356
S(1)–Cl(6)	3.249 (2)	3.129 (3)	3.138 (9)	3.219
S(1)–Cl(6)′	3.249 (2)	3.119 (3)	3.142 (9)	3.138
		Bond Angles		
Cl(1)–S(1)–Cl(2)	104.4 (1)	101.9 (1)	101.4 (4)	101.7 (7)
Cl(2)–S(1)–Cl(2)′	102.2 (1)	100.7 (1)	101.1 (4), 103.5 (4)	103.5 (7), 101.8 (6)
Cl(3)–Sb(1)–Cl(4)	90.0 (0)			
Cl(3)–Sb(1)–Cl(5)	90.0 (0)			
Cl(4)–Sb(1)–Cl(5)	87.99 (8)			
Cl(4)–S(1)–Cl(1)	152.62 (9)	154.9 (1)	165.4	154.9
Cl(6)–S(1)–Cl(2)	163.4 (1)	156.4 (1)	156.8	158.9
Cl(6)–S(1)–Cl(2)	163.4 (1)	167.2 (1)	161.8	159.7

[a] Reference 21a [b] Reference 21c. [c] Reference 21b. [d] In $(SCl_3^+)(AsF_6^-)$ the S–Cl distances are 1.949, 1.972, and 1.988 Å (no esd's), and the average S···F contact distance is 2.90 Å.[21d] [e] Distances in the anion (Å): Sb–Cl(3), 2.313 (2); Sb–Cl(4), 2.363 (2); Sb–Cl(5), 2.355 (2); Sb–Cl(6), 2.363 (2); Sb–Cl(7), 2.352 (2).

The two hexachloroantimonate anions in the structure are nearly octahedral, with Sb–Cl bond lengths of 2.375 Å (×6) and 2.369 Å (×6).

3. $(SeCl_3^+)(SbCl_6^-)$. This compound is isomorphous with $(SBr_{1.2}Cl_{1.8}^+)(SbCl_6^-)$ although the $SeCl_3^+$ cation is now almost equally disordered over two selenium positions (population pa-

Table V. Geometries of the Primary and Secondary Bonding Arrangements in Salts of the Trihalochalcogen Cations, MX_3^+[s]

	M-X, Å	M-Y, Å	X···Y, Å	X-M-X, deg	X-M-Y, deg	M-X···Y, deg
$(SF_3^+)(BF_4^-)$[a]	1.495 (2) (×2)	2.593 (3)		97.62 (7)	178.1 (1)	
	1.499 (2)	2.624 (2) (×2)		97.39 (12) (×2)	171.5 (1) (×2)	
SeF_4[b]	1.679	2.661		96.9, 85.5	171.0	
	1.669	2.653		85.7, 87.5	169.5	
	1.792	1.802			169.3	
	σ ~ 0.006			σ ~ 0.3		
(SeF_3^+)-	1.69	2.33		93.3	174.0	
(NbF_6^-)[c]	1.72	2.41		94.0	175.9	
	1.77	2.24		98.2	176.2	
	1.73 (×3)	2.43 (×3)		94.1	176.6	
	σ ~ 0.04			σ ~ 2–3		
(SeF_3^+)-	1.64	2.42		93.9	171.5	
$(Nb_2F_{11}^-)$[c]	1.66	2.47		94.1	171.5	
	1.67	2.40		94.6	174.3	
	σ ~ 0.02			σ ~ 0.4		
TeF_4[b]	1.830	~2.94, 3.01, 3.36		86.8	161.3	
	1.874	2.284		87.6	162.5	
	1.893	2.078		84.2		
	σ ~ 0.005			σ ~ 0.2		
(TeF_3^+)-	1.83 (5)	2.55 (3), 2.94 (4)		88 (2)	162 (2)	
$(Sb_2F_{11}^-)$[d]	1.86 (4)	2.69 (3), 3.51 (4)		90 (2)	158 (1)	
	1.83 (3)	2.54 (3), 3.55 (4)		93 (2)	159 (1)	
$(TeF_3)_2SO_4$[e]	1.837 (8)	3.13 (1), 3.321 (8)		86.5 (4), 86.5 (5)		
		3.303 (8), 3.079 (8)		80.8 (4), 79.1 (4)		
	1.860 (8)	2.32 (1)		87.8 (4), 86.5 (4)	163.2 (4)	
	1.900 (8)	2.213 (9)		82.8 (4)	166.4 (4)	
	1.845 (8)	2.668 (9), 3.16 (1), 3.27 (1)		89.4 (4), 89.1 (4)		
				82.3 (4), 80.7 (4)		
	1.850 (8)	2.342 (11)		85.3 (4), 73.8 (4)	164.8 (4)	
	1.857 (9)	2.374 (10)		81.8 (4)	156.8 (4)	
$(SCl_3^+)(ICl_4^-)$[f]	2.002 (3)	3.097 (3)		100.7 (1)	154.9 (1)	
	1.986 (3)	3.129 (3)		101.9 (1)	156.4 (1)	
	1.977 (3)	3.119 (3)		101.2 (1)	167.2 (1)	
(SCl_3^+)-	1.954 (3)	3.164 (4)		104.4 (1) (×2)	152.7 (1)	
$(SbCl_6^-)$[e]	1.957 (2) (×2)	3.248 (2) (×2)		102.2 (1)	163.5 (1) (×2)	
(SCl_3^+)-	1.955 (14)	3.356		101.7 (7)	154.9	
(UCl_6^-)[g]	1.973 (13)	3.219		103.5 (7)	158.9	
	1.959 (12)	3.138		101.8 (6)	159.7	
$(SBr_{1.2}Cl_{1.8}^+)$-	2.077 (2) (×3)	3.313 (2) (×3)		105.3 (1) (×3)	149.1 (1) (×3)	
$(SbCl_6^-)$[e]	2.039 (4) (×3)	3.232 (4) (×3)		108.1 (1) (×3)	147.6 (1) (×3)	
α-$SeCl_4$[h]	2.146	2.874		95.6	173.5	
	2.166	2.766		95.6	170.0	
	2.160	2.924		96.1	169.0	
	2.174 (×3)	2.820 (×3)		96.3 (×3)	171.8 (×3)	
	σ ~ 0.005			σ ~ 0.2		
β-$SeCl_4$[h]	2.169 (2.169)	2.766 (2.769)		96.8 (96.6)	172.0 (171.9)	
	2.156 (2.150)	2.791 (2.818)		94.5 (97.0)	171.0 (171.7)	
	2.186 (2.150)	2.761 (2.859)		95.1 (96.6)	173.0 (169.9)	
	σ ~ 0.005			σ ~ 0.2		
$(SeCl_3^+)$-	2.11 (2.12)	3.05 (3.05)		99.3 (100.0)	165.0 (165.8)	
$(AlCl_4^-)$[i]	2.07 (2.11)	3.03 (3.03)		99.4 (98.9)	171.4 (166.3)	
	2.13 (2.13)	3.11 (2.97)		99.1 (99.3)	166.3 (170.2)	
	σ ~ 0.01			σ ~ 0.4		
$(SeCl_3^+)$-	2.146 (2)	2.883 (2)		no angles given		
$(MoOCl_4^-)$[j]	2.149 (2)	2.909 (2)				
	2.150 (2)	2.841 (2)				
$(SeCl_3^+)$-	2.09 (1) (×3)	3.14 (1) (×3)		102.5 (4) (×3)	154.0 (4) (×3)	
$(SbCl_6^-)$[l]	2.10 (1) (×3)	3.12 (1) (×3)		103.6 (4) (×3)	153.1 (4) (×3)	
β-$(TeCl_3^+)$-	2.279 (2.278)	3.041 (3.065)		94.9 (96.0)	173.1 (177.3)	
$(AlCl_4^-)$[e,k]	2.281 (2.273)	3.086 (3.043)		94.4 (96.0)	177.4 (171.1)	
	2.277 (2.275)	3.067 (3.150)		95.0 (95.0)	177.1 (172.8)	
	σ ~ 0.002			σ ~ 0.1		

Table V (Continued)

	M-X, Å	M-Y, Å	X···Y, Å	X-M-X, deg	X-M-Y, deg	M-X···Y, deg
α-$(TeCl_3^+)$-	2.282	3.042		95.6	177.3	
$(AlCl_4^-)^{e,k}$	2.274	3.013		95.1	177.4	
	2.272	3.129		94.4	176.3	
	$\sigma \sim 0.002$			$\sigma \sim 0.1$–0.2		
$TeCl_4^l$	2.315 (2.313)	2.898 (2.916)		95.7 (94.9)	173.1 (174.0)	
	2.312 (2.314)	2.947 (2.944)		93.7 (95.1)	171.6 (173.6)	
	2.317 (2.296)	2.908 (2.959)		94.2 (95.0)	174.2 (171.5)	
	$\sigma \sim 0.003$			$\sigma \sim 0.1$–0.2		
$(TeCl_3^+)$-	2.261 (2) (×2)	2.778 (4) (×2)		97.6 (1) (×2)	167.6 (1)	
$(SbF_6^-)^e$	2.252 (3)	2.660 (6) (Te···F)		92.3 (1)	175.0 (2)	
		2.950 (6)				
$(TeCl_3^+)$-	2.258 (2)	2.962 (6)		95.7 (1)	169.5 (1)	
$(AsF_6^-)^e$	2.266 (2)	2.738 (5)		96.7 (1)	178.7 (1)	
	2.268 (2)	2.689 (4) (Te···F)		95.7 (1)	176.4 (1)	
		3.149 (6), 3.259 (5)				
$(SeBr_3^+)$-	2.272 (8)	2.76 (3)	3.02 (5)	103.3 (3)	155.2 (9)	161 (1)
$(SbF_6^-)^m$	2.254 (7)	2.72 (4)	2.85 (5)	99.0 (3)	171.0 (9)	169 (1)
	2.280 (8)	2.83 (4)	3.02 (5)	100.4 (3)	177.7 (8)	159 (1)
α-$SeBr_4^n$	2.35 (2.35)	3.02 (3.02)		94.2 (98.5)	174.7 (167.6)	
	2.31 (2.37)	3.05 (2.93)		96.8 (97.8)	169.6 (168.0)	
	2.44 (2.33)	2.87 (3.01)		95.2 (98.8)	172.2 (170.5)	
	2.38 (2.34) (×3)	2.92 (3.01) (×3)		95.8 (93.9) (×3)	170.6 (168.1) (×3)	
	$\sigma \sim 0.03$			$\sigma \sim 0.5$–1.0		
$(TeBr_3^+)$-	2.428 (2)	2.80 (1)	3.34 (1)	95.9 (1)	173.1 (2)	162.1 (2)
$(AsF_6^-)^m$	2.438 (3)	2.78 (1)	3.07 (1)	99.5 (1)	172.9 (3)	145.2 (3)
	2.430 (2)	2.93 (1)	3.05 (1)	98.4 (1)	175.5 (3)	87.6 (3)
		3.40 (1)				
(TeI_3^+)-	2.663 (1)	2.88 (1)	3.11 (1)	103.40 (5)	170.2 (5)	151.3 (5)
$(AsF_6^-)^o$	2.665 (2)	2.90 (1)	...	100.86 (5)	172.6 (5)	...
	2.674 (2)	3.16 (1)	3.04 (1)	95.42 (5)	173.5 (5)	165.3 (5)
(Ph_3C^+)-	2.326 (2.347)	2.924 (2.774)		92.6 (97.1)	173.2 (170.8)	
$(Te_3Cl_{13}^-)^p$	2.337 (2.335)	2.824 (2.863)		92.6 (90.4)	176.3 (178.1)	
	2.349 (2.320)	2.788 (2.941)		93.6 (93.7)	174.1 (177.0)	
	2.388 (2.355)	2.706 (2.763)		90.4 (94.2)	177.7 (171.4)	
	2.323	2.984		92.3	170.1	
	$\sigma \sim 0.005$			$\sigma \sim 0.1$–0.2		
$[PCl_4^+$-	2.345 (2.357)	2.829 (2.852)		88.8 (87.8)	179.2 (171.7)	
$TeCl_5^-]_n^q$	2.498 (2.489)	2.498 (2.489)		86.9 (88.3)	173.2 (174.2)	
	2.375 (2.382)	2.783 (2.693)		92.3 (93.9)	178.7 (179.1)	
	$\sigma \sim 0.005$			$\sigma \sim 0.1$–0.2		
TeI_4^r	2.753 (×2)	3.279 (×2)		96.76 (×2)	169.04	
	2.772	3.200		95.35	172.46 (×2)	
	2.766	3.247		93.99	173.42	
	2.770	3.241		91.20	173.96	
	2.933	2.989		95.28		
	2.761	3.214		91.90	176.50	
	2.789 (×2)	3.331 (×2)		91.64	173.70 (×2)	
	$\sigma \sim 0.001$			95.51	170.37	
				95.54 (×2)		

[a] Gibler, D. D.; Adams, C. J.; Fischer, M.; Zalkin, A.; Bartlett, N. *Inorg. Chem.* **1972**, *11*, 2325. [b] Reference 36. SeF_4 has an $AX_4Y'_2E$ geometry; TeF_4 has an AX_5Y_3E geometry. [c] Edwards, A. J.; Jones, G. R. *J. Chem. Soc. A* **1970**, 1491 and 1891. [d] Reference 34. Te has an $AX_3Y_3Y'_3E$ geometry. [e] This work. $(TeF_3)_2(SO_4)$: Te(1), AX_5Y_4E; Te(2), AX_5Y_3E. $(TeCl_3)(SbF_6)$: $AX_3Y_3Y'E$. $(TeCl_3)(AsF_6)$: $AX_3Y_3Y'_2E$, otherwise geometries are AX_3Y_3E type. [f] Reference 21. [g] Reference 22. [h] Born, P.; Kniep, R.; Mootz, D. *Z. Naturforsch, B: Anorg. Chem., Org. Chem.* **1981**, *36B*, 1516. Kniep, R.; Korte, L.; Mootz, D. *Ibid.* **1981**, *36B*, 1660. [i] Reference 27. [j] Reference 28. [k] Reference 3. [l] Reference 29. [m] Reference 26. [n] Born, P.; Kniep, R.; Mootz, D. *Z. Anorg. Allg. Chem.* **1979**, *451*, 12. [o] Reference 39. [p] Reference 30. [q] Reference 31. [r] Krebs, B.; Paulat, V. *Acta Crystallogr., Sect. B: Struct. Crystallogr. Cryst. Chem.* **1976**, *B26*, 1470. [s] Geometries are AX_3Y_3E unless indicated in footnotes. Trans-related distances are given.

rameters 0.426 (4) and 0.480 (4)) resulting in equivalent Se–Cl distances (2.09 (1) and 2.10 (1) Å (both ×3)) and Cl–Se–Cl angles (102.5 and 103.6 (4)°) (Table V). These Se–Cl bonds are comparable in length to those in $(SeCl_3^+)(AlCl_4^-)$,[27] but are significantly shorter than the Se–Cl bonds in $(SeCl_3^+)(MoOCl_4^-)$ (where the secondary contacts are slightly stronger[28] (Table V)). The AX_3Y_3E geometry of each Se position is completed by 3 secondary Se···Cl contacts of lengths 3.14 (1) (Se(1)···Cl(3) (×3)) and 3.12 (1) Å (Se(2)···Cl(2) (×3)) approximately trans to the primary

---

(27) Stork-Blaisse, B. A.; Romers, C. *Acta Crystallogr., Sect. B: Struct. Crystallogr. Cryst. Chem.* **1971**, *B27*, 386.

(28) Gleizes, A.; Galy, J. P. *C. R. Seances Acad. Sci., Ser. C* **1978**, *286*, 29.

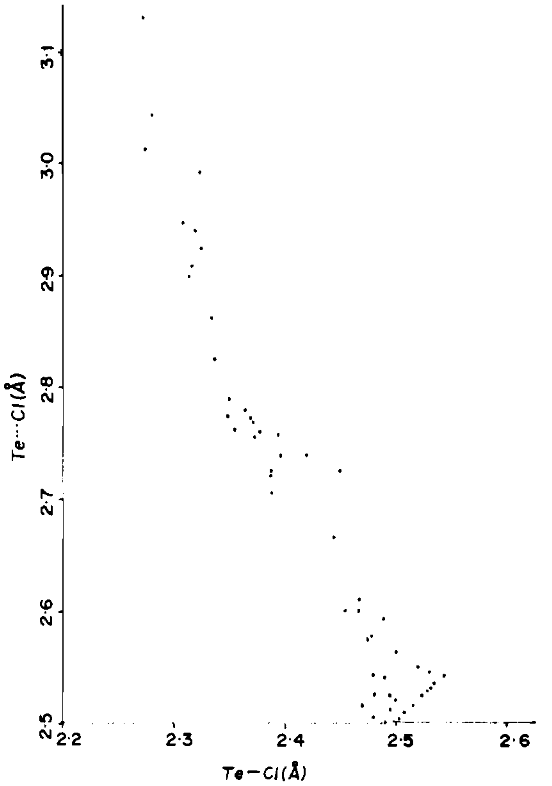

Figure 1. Correlation between trans-related Te–Cl primary and Te···Cl secondary bond lengths.

bonds (Cl–Se···Cl angles are 154.0 (4) and 153.1 (4)°). The hexachloroantimonate anions are octahedral with Sb–Cl distances 2.369 (6) Å (×6) and 2.382 (5) Å (×6).

4. $(TeCl_3^+)(AlCl_4^-)$. Crystals isolated from the reaction of S_7TeCl_2 with $AlCl_3$ are a new (β) form of $(TeCl_3)(AlCl_4)$. The previously reported (α) form of this compound is monoclinic, space group $C2/c$ with one ion pair in the asymmetric unit.[3] In the present triclinic ($P\bar{1}$) form the dimensions of the two independent $TeCl_3^+$ and $AlCl_4^-$ ions differ significantly from one another and from those of the equivalent ions in the α modification (Table V) due to appreciable anion–cation interactions in both $TeCl_3^+$ structures. Overall the geometry of each tellurium atom in β-$(TeCl_3)(AlCl_4)$ is a distorted monocapped octahedron AX_3Y_3E with average Te–Cl and Te···Cl distances of 2.277 and 3.074 Å. In the present salts, as well as other Te(IV) structures including $TeCl_4$,[29] the anions $Te_3Cl_{13}^-$ [30] and $(TeCl_5^-)_n$,[31] and examples of the $TeCl_6^{2-}$ anion,[32] when the primary Te–Cl bond lengths are plotted against the approximately trans-related secondary bond lengths they fall on a smooth curve (Figure 1). This is consistent with the proposed charge-transfer model.[1]

As a result of the Te···Cl interactions, the packing of the triclinic modification consists of spiral columns of anions and cations along a. In the α form of $(TeCl_3^+)(AlCl_4^-)$ the packing is in the form of layers. Each layer is a network of six-membered rings of alternating $TeCl_6$ octahedra and $AlCl_4$ tetrahedra.[3]

Bond angles in the $TeCl_3^+$ cations are 94.4–96.0 (1)° in the triclinic modification and 94.4–95.6 (2)° in the monoclinic form. These angles are significantly smaller than the bond angles in $SeCl_3^+$ and SCl_3^+ (Table V). Furthermore the *trans*-X–A–Y angles in the $TeCl_3^+$ cations, which are 171.1–177.3 (1)° (β) and 176.3–177.4 (2)° (α) are significantly closer to 180° than related angles in the $SeCl_3^+$ (e.g. 165–171° in $(SeCl_3)^+(AlCl_4^-)$[27]) and SCl_3^+ cations (153–167°) (Table V).

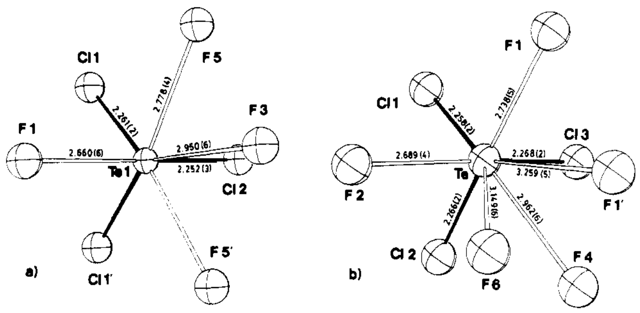

Figure 2. The $TeCl_3^+$ cation in (a) $(TeCl_3)(SbF_6)$, an example of $AX_3Y_3Y'E$ geometry, and (b) $(TeCl_3)(AsF_6)$, an $AX_3Y_3Y'_2E$ geometry. Both views are toward the assumed position of the lone pair of electrons on tellurium.

The two tetrachloroaluminate anions are both slightly flattened tetrahedra with one bond 0.04–0.05 Å shorter than the rest. The shorter bonds are to chlorine atoms not involved in any significant Te···Cl interactions. In the α form of $(TeCl_3)(AlCl_4)$ the anion also forms three Al–Cl distances to bridging chlorine atoms of 2.138–2.146 Å and the fourth Al–Cl bond to a noncoordinating atom of 2.087 Å.[3] The correlation between Al–Cl bond lengths and Cl–Al–Cl bond angles in the present anions is consistent with that discussed in ref 33.

5. $(TeCl_3^+)(SbF_6^-)$ and $(TeCl_3^+)(AsF_6^-)$. These two salts were found to be nonisomorphous, as the hexafluoroantimonate salt crystallizes in the orthorhombic space group $Pnma$, while the hexafluoroarsenate salt crystallizes in the monoclinic space group $P2_1/n$. It is noteable that the corresponding salts $(SeBr_3)(SbF_6)$ (orthorhombic, space group $P2_12_12_1$) and $(SeBr_3)(AsF_6)$ (monoclinic, space group $P2_1/c$) are also not isomorphous.[26]

In $(TeCl_3)(SbF_6)$ the cation has crystallographic mirror symmetry and is significantly distorted from C_{3v} symmetry with Cl–Te–Cl angles of 97.6 (1) (×2) and 92.3 (1)°. Furthermore, the Te–Cl distances of 2.261 (2) (×2) and 2.252 (3) Å are significantly shorter than those for β-$(TeCl_3^+)(AlCl_4^-)$ (mean 2.277 (2) Å) or $TeCl_4$ (mean 2.311 (3) Å).[29] These differences can be correlated with the strengths of the interionic contacts involving each $TeCl_3^+$ cation. As discussed above, the Te–Cl primary bond length is seen to increase as the Te···Cl secondary bond in a direction approximately trans to the primary bond decreases in length (Figure 1). In the present salt there are three Te···F contacts shorter than van der Waals distances that cap the Cl–Cl–E faces and a fourth contact that bridges a Cl–E edge of the $TeCl_3E$ tetrahedron to give an overall $AX_3Y_3Y'E$ arrangement (Figure 2). The face-capping Te···F contacts (2.660 (6) and 2.778 (4) Å (×2)) are weak compared to some of the Te···Cl contacts in other $TeCl_3^+$ salts but are consistent with the short Te–Cl primary bond lengths observed and with the correlation observed in Figure 1 (cf. also the structure of $SCl_3^+AsF_6^-$ discussed above). In comparison, the Te···F contacts in $(TeF_3)(Sb_2F_{11})$, which has an $AX_3Y_3Y'_3E$ tricapped trigonal prismatic arrangement of ligands, are 2.54 (3), 2.55 (3), 2.69 (3), 2.94 (4), 3.51 (4), and 3.55 (4) Å.[2,34] This difference in secondary bond strengths for F and Cl ligands is a function of size and polarizability (Cl > F). The additional edge-bridging contact (2.950 (6) Å) may force atoms $F(5^{II})$ and $F(5^{V})$ apart, reducing the Cl(1)–Te···F(5) angles to 167.6 (1)° (×2) (cf. Cl(2)–Te···F(1) = 175.0 (2)°) and perhaps influencing the Cl(1)–Te–Cl(2) primary bond angles of 97.6 (1)° (×2) (Table V).

The hexafluoroantimonate anion, with crystallographic symmetry m is a distorted octahedron in which the Sb–F bond lengths to atoms involved in the shortest Te···F contacts (1.879 (5), 1.863 (6), and 1.867 (4) Å) are slightly longer than those to atoms that do not form any contacts (1.842 (7) and 1.843 (4) Å). The

---

(29) Buss, B.; Krebs, B. *Inorg. Chem.* **1971**, *10*, 2795.

(30) Krebs, B.; Paulat, V. *Z. Naturforsch, B: Anorg. Chem., Org. Chem.* **1979**, *34B*, 900.

(31) Krebs, B.; Buss, B.; Berger, W. *Z. Anorg. Allg. Chem.* **1973**, *397*, 1.

(32) Khodadad, P.; Viossat, B.; Toffoli, P.; Rodier, N. *Acta Crystallogr., Sect. B: Struct. Crystalogr. Cryst. Chem.* **1979**, *B35*, 2896. von Deuten, K.; Schnabel, W.; Klar, G. *Cryst. Struct. Commun.* **1980**, *9*, 761. Russo, U.; Calogero, S.; Valle, G. *Ibid.* **1980**, *9*, 829. Ault, H. K.; Husebye, S. *Acta Chem. Scand., Ser. A* **1978**, *A32*, 157.

(33) Murrey-Rust, P.; Burgi, H. B.; Dunitz, J. D. *Acta Crystallogr., Sect. B: Struct. Crystallogr. Cryst. Chem.* **1978**, *B34*, 1793.

(34) Edwards, A. J.; Taylor, P. *J. Chem. Soc., Dalton Trans.* **1973**, 2150.

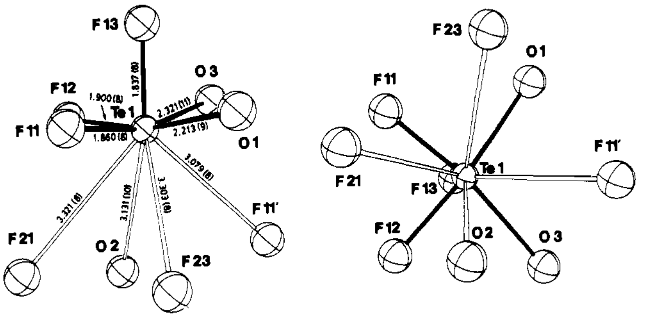

Figure 3. Two views of Te(1) in $(TeF_3)_2(SO_4)$ showing secondary bonds (unfilled bonds) capping X–X–E faces of the AX_5E polyhedron, giving an overall AX_5Y_4E geometry.

F–Sb–F_{cis} angles for these interacting atoms are all slightly less than 90°.

In $(TeCl_3)(AsF_6)$ the Cl–Te–Cl bond angles of 95.7 (1), 95.7 (1), and 96.7 (1)° show that the cation is much less distorted from C_{3v} symmetry than in the hexafluoroantimonate salt, although the average bond angle in the two salts is virtually the same (95.8 (SbF_6^-) and 96.0° (AsF_6^-)). There is very little difference in the Te–Cl bond lengths for both salts. Any differences are due to the additional secondary interactions to each Te atom. In $(TeCl_3)(AsF_6)$ of the five Te···F interactions less than van der Waals limits (3.55Å) three are approximately trans to the Te–Cl primary bonds (Cl–Te···F angles of 169.5 (1), 176.4 (1), and 178.7 (1)°) and are face capping the $TeCl_3E$ tetrahedron. Two further longer interactions approximately bridge Cl–E edges of the same tetrahedron (Figure 2). Overall the environment of the Te may be designated as $AX_3Y_3Y'_2E$.

The hexafluoroarsenate anion is a distorted octahedron with As–F bond lengths of 1.663 (5)–1.730 (5) Å, *cis*-F–As–F angles of 87.4 (3)–93.6 (3)°, and *trans*-F–As–F angles of 175.6 (3)–178.9 (3)°. The longer As–F bonds are again to those atoms involved in the shortest Te···F interactions.

6. $(TeF_3)_2(SO_4)$. In this salt the distinction between an ionic sulfate and a covalently linked sulfate cannot be made with certainty since anion–cation Te···O distances are as short as 2.213 (9) Å. Each Te atom forms two short Te–O bonds so that the primary geometry of these atoms may be considered to be distorted square-pyramidal AX_5E with the lone pair in the remaining octahedral position and trans to the shorter Te(1)–F(13) and Te(2)–F(23) axial bonds of lengths 1.837 (8) and 1.845 (8) Å. The remaining Te–F bond lengths then appear to be a function of the strength of the trans-related Te–O distances (Table V, Figure 3). For comparison the Te–F bond lengths in $(TeF_3)(Sb_2F_{11})$ are 1.83 (3), 1.83 (5), and 1.86 (4) Å,[34] and in the square-pyramidal TeF_5^- ion the Te–F bond lengths are 1.84 (2) (axial) and 1.96 (2) Å (×4) (equatorial).[35]

Completing the overall coordination out to the van der Waals limits in $(TeF_3)_2(SO_4)$ are four contacts to Te(1) and three contacts to Te(2) (Figure 3), which approximately cap faces of the AX_5E octahedron describing the primary geometry. Overall the geometry of Te(1) can be described as AX_5Y_4E and that of Te(2) as AX_5Y_3E. Similar arrangements of primary and secondary bonds based on AX_5E primary geometries are common in compounds containing the XeF_5^+ cation.[2]

Alternatively, if the Te···O distances of 2.2–2.3 Å are not considered as primary bonds, then for Te(1) the overall arrangement of three primary and six secondary bonds around the lone pair E could be described as $AX_3Y_3Y'_3E$ as has been observed for $(TeF_3)(Sb_2F_{11})$.[2] (Te(2) would be described as $AX_3Y_3Y'_2E$). From Figure 4 it can be seen that the $AX_3Y_3Y'_3E$ arrangement changes to the AX_5Y_4E arrangement as the two face-capping contacts Y_1 and Y_2 in the $AX_3Y_3Y'_3E$ situation shorten to primary bonding distances, forcing the lone pair E into a position approximately trans to the AX_1 axial bond and three edge-bridging contacts Y'_1, Y'_2, and Y'_3 into the face capping contacts Y_1, Y_2, and Y_4 of the AX_5Y_4E arrangement.

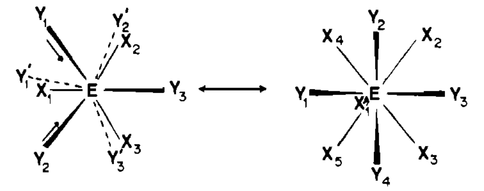

Figure 4. Interrelationship between $AX_3Y_3Y'_3E$ and AX_5Y_4E geometries.

Table VI. Bond Valence Sums in Te(IV)–F/O Compounds

$(TeF_3)_2(SO_4)$		$(OOs(OTeF_5)_4TeF_3^+)(F^-)\cdot 2TeF_4$	
Te(1)	4.01	Te(5)	3.91
Te(2)	3.90	Te(6)	3.95
TeF_4	4.00	Te(7)	4.10
$KTeF_5$	3.74	$(TeF_3)(Sb_2F_{11})$	3.83

The environments of the Te(IV) atoms in TeF_4[36] and $(OOs(OTeF_5)_4TeF_3^+)(F^-)\cdot 2TeF_4$[37] are comparable to the present Te environments. In TeF_4 the Te atom has a distorted AX_5E square-pyramidal arrangement of ligands cis bridged to form endless chains (Te–F = 1.80 (2) (axial), 1.87 (3)–2.26 (3) Å (equatorial)). Completing the overall environment are three Te···F secondary bonds (2.94 (3), 3.01 (3), and 3.36 (2) Å) capping three faces of the TeF_5E octahedron containing the lone pair as a vertex (AX_5Y_3E). Two of the Te(IV) atoms in the osmium compound have trigonal-bipyramidal AX_4E primary geometries. A third Te atom has a primary geometry intermediate between trigonal-bipyramidal AX_4E and octahedral AX_5E depending on whether a Te···F distance of 2.40 Å is considered a primary bond or not. All three Te atoms are involved in further weak secondary Te···F interactions. From the bond valence equations $S = S_0(R/R_0)^{-N}$ with $S_0 = 1$, $R_0 = 1.779$, and $N = 3.5$ for Te(IV)–F and $S_0 = 1.333$, $R_0 = 1.813$ and $N = 4.5$ for Te(IV)–O interactions,[38] individual bond valencies for the "bonds" from the Te(IV) atoms in the compounds above to all F or O atoms within the van der Waals limits were calculated. The total valence sums (Table VI) are reasonably close to the theoretical value of 4.0. This argues in favor of the inclusion of these longer interactions in the overall description of the geometry around tellurium.

Anion–Cation Interactions and the Geometry of MX_3^+ Cations

The bond lengths in the group VI (group 16[47]) MX_3^+ cations are in every case shorter and the XMX bond angles slightly larger than the corresponding values in the isoelectronic group V (group 15) trihalide molecules[26] (Table V). The shorter bond lengths in the cations are consistent with the smaller covalent radii of the group VI atoms, which will be further decreased by their formal positive charge. Thus the bonding electron pairs in the shorter bonds of the MX_3^+ cation will be closer and therefore repel each other more strongly than in the neutral group V molecules, leading to the larger observed bond angles.

For a given group V or VI atom M it is observed that the X–M–X angle increases in the order F < Cl < Br < I. This is consistent with the changing electronegativity of X (F > Cl > Br > I), since the greater the electronegativity of X, the more X contracts the charge cloud of the bonding pair and attracts it to itself, thus reducing bp–bp repulsions and decreasing the angle X–M–X. For example, X–Te–X is 90 (2)° in $(TeF_3)(Sb_2F_{11})$,[34] 96.0 (1)° in $(TeCl_3)(AsF_6)$, 97.82 (8)° in $(TeBr_3)(AsF_6)$,[26] and 99.9 (1)° in $(TeI_3)(AsF_6)$.[39]

In the series of cations MF_3^+ and MCl_3^+ (or the equivalent group V neutral molecules) the increasing size of M (S < Se < Te) allows the lone pair of electrons to spread out further on the

---

[35] Mastin, S. H.; Ryan, R. R.; Asprey, L. B. *Inorg. Chem.* **1970**, *9*, 2100.

[36] Edwards, A. J.; Hewaidy, F. I. *J. Chem. Soc. A* **1968**, 2977. Kneip, R.; Korte, L.; Kryschi, R.; Poll, W. *Angew. Chem., Int. Ed. Engl.* **1984**, *23*, 388.

[37] Huppmann, P.; Labischinski, H.; Lentz, D.; Pritzkow, H.; Seppelt, K. *Z. Anorg. Allg. Chem.* **1982**, *487*, 7.

[38] Brown, I. D. *J. Solid State Chem.* **1974**, *11*, 214.

[39] Passmore, J.; Sutherland, G.; White, P. S. *Can. J. Chem.* **1981**, *59*, 2876.

Table VII. Raman Spectra of $(MCl_3)(SbCl_6)$ (M = S, Se, Te) and $(SBr_{1.2}Cl_{1.8})(SbCl_6)$

$(SCl_3)(SbCl_6)$		$(SeCl_3)(SbCl_6)$		$(TeCl_3)(SbCl_6)$		$(SBr_{1.2}Cl_{1.8})(SbCl_6)$[a]	
band, cm^{-1} (rel intens)	assignt	band, cm^{-1} (rel intens)	assignt	band, cm^{-1} (rel intens)	assignt	band, cm^{-1} (rel intens)	assignt
535 (63)	SCl_3^+, $\nu_3(E)$	396 (sh)	$SeCl_3^+$, $\nu_3(E)$	381 (47)	$TeCl_3^+$, $\nu_3(E)$	411 (21)	SBr_3^+, $\nu_3(E)$
521 (48)						389 (31)	
500 (99)	SCl_3^+, $\nu_1(A)$	407 (100)	$SeCl_3^+$, $\nu_1(A)$	395 (100)	$TeCl_3^+$, $\nu_1(A)$	371 (33)	SBr_3^+, $\nu_1(A)$
336 (79)	$SbCl_6^-$, $\nu_1(A_{1g})$	353 (20)	$SbCl_5$?[b]	355 (28)	$SbCl_5$?[b]		
328 (100)		318 (43)	$SbCl_6^-$, $\nu_1(A_{1g})$	309 (84)	$SbCl_6^-$, $\nu_1(A_{1g})$	333 (100)	$SbCl_6^-$, $\nu_1(A_{1g})$
294 (21)	$SbCl_6^-$, $\nu_2(E_g)$	277 (16)	$SbCl_6^-$, $\nu_2(E_g)$	254 (25)	$SbCl_6^-$, $\nu_2(E_g)$	286 (28)	$SbCl_6^-$, $\nu_2(E_g)$
286 (33)							
275 (27)	SCl_3^+, $\nu_2(A)$	198 (21)	$SeCl_3^+$, $\nu_2(A)$			242 (10)	SCl_2Br^+, $\nu_3(A')$[c]
266 (5)	?			186 (18)		209 (30)	$SClBr_2^+$, $\nu_3(A')$[c]
216 (11)	SCl_3^+, $\nu_4(E)$	184 (36)	$SeCl_3^+$, $\nu_4(E)$; $SbCl_6^-$, $\nu_5(T_{2g})$	176 (28)	$TeCl_3^+$, $\nu_2(A)$; $TeCl_3^+$, $\nu_4(E)$; $SbCl_6^-$, $\nu_5(T_{2g})$	182 (54)	SBr_3^+, $\nu_2(E)$; $SbCl_6^-$, $\nu_5(T_{2g})$
208 (23)		169 (17)		169 (39)		176 (75)	
175 (72)	$SbCl_6^-$, $\nu_5(T_{2g})$	162 (26)		163 (37)		163 (23)	
166 (9)		130 (16)		146 (25)		133 (23)	SBr_3^+, $\nu_4(E)$
						123 (41)	

[a] SCl_3^+ peaks not listed. [b] Reference 42. [c] Reference 43.

surface of the central atom, thus pushing the bond pairs together so that the X–M–X angle between the bonding pairs decreases from S to Se to Te in both series (Table V). Similarly, the Br–M–Br angle is smaller in $(TeBr_3)(AsF_6)$ than in $(SeBr_3)(SbF_6)$.[26] The stereoactivity of the lone pair in these series with respect to the primary bonds can also be examined by using a hybridization model. The increasing s–p energy separation in going down a group leads to the lone pair on Te having more s character than the lone pair on S. As a consequence, the M–X primary bonds involving Te have more p character and correspondingly smaller angles.

Secondary bonding trends are consistent with these observations on the size and stereoactivity of the lone pair with respect to the arrangements of the primary bonds, in that these weaker interactions avoid the lone pair as much as possible while at the same time maximizing the overlap with antibonding orbitals of the M–X primary bonds. Therefore they tend to surround the lone pair and are frequently found in positions approximately trans to the primary bonds or else along an edge of the polyhedron describing the primary geometry that contains the lone pair at one end.[2] Generally secondary bonding in the neutral group V trihalide molecules is weaker than in the MX_3^+ salts. Furthermore, since secondary bonds overlap with antibonding orbitals of the M–X primary bonds, stronger secondary bonding weakens the primary bonds, leading to a decrease in any bp–bp repulsions with respect to the lp–bp repulsions and hence smaller X–M–X angles. Thus the angle expansion on going from a neutral molecule to an MX_3^+ cation may be small. For example, the Cl–P–Cl mean angle in PCl_3 is 100.09 (9)° and the intermolecular contacts are all greater than the usual van der Waals distance,[2,40] whereas the mean Cl–S–Cl angles in $(SCl_3)(ICl_4)$ and $(SCl_3)(SbCl_6)$ are 101.3 (1) and 103.7 (2)°, respectively. As noted above, the significant difference between the two Cl–S–Cl angles is consistent with the different strengths of the secondary bonds to each sulfur.

From the above, the stereoactivity of the lone pair with respect to any secondary bonding is inversely related to its stereoactivity with respect to the primary bonds; that is, as the lone pair spreads out further on the surface of the central atom M it has more s character and its radial extent in the directions in which the secondary bonds form decreases. Thus the strength of the secondary bonding interactions M···Y increases in the series S < Se < Te, consistent with the increasing electropositive nature of the chalcogen atom in the same order (Table V). For example, M···Y is 3.220 (3), 3.13 (1), and 3.075 (2) Å or 0.35, 0.52, and 0.73 Å, respectively, less than van der Waals limiting distances in $(SCl_3)(SbCl_6)$, $(SeCl_3)(SbCl_6)$ and β-$(TeCl_3)(AlCl_4)$ (Table V).

For a given M, the tendency for contacts to X to become significant increases in the order F < Cl << Br < I, corresponding to the increasing polarizability and electropositive nature of X in the same series. In the structures reported in this paper this type of contact is not common, but it can be seen in $(TeI_3)(AsF_6)$,[39] $(TeBr_3)(AsF_6)$,[26] and $(SeBr_3)(SbF_6)$.[26] Consistent with the increase in strength of the contacts to X there is a tendency for the contacts to M to simultaneously decrease in strength; that is, the degree of charge-transfer to the cation via both the M···Y and X···Y contacts appear to be approximately constant. Thus in $(TeF_3)(Sb_2F_{11})$, $(TeCl_3)(SbF_6)$, $(TeBr_3)(AsF_6)$, and $(TeI_3)(AsF_6)$, the M···Y contact steadily increases in length (2.59 (3) → 2.738 (5) → 2.84 (1) → 2.98 (1) Å, respectively) while for $(TeBr_3^+)$ and (TeI_3^+) the shortest X···Y contacts are 3.05 (1) and 3.04 (1) Å, respectively. These trends are, however, conditional on the overall environment of the central atom remaining essentially the same in each series of compounds. In this respect, the size of the Y atoms is of importance, and when the anion contains fluorine or oxygen atoms, more complicated environments than AX_3Y_3E monocapped octahedra may be observed. In the examples with F or O atoms in the anion the charge transfer to M is shared among several interactions so that individual M···F distances are longer in $(TeCl_3)(SbF_6)$, for example, than the M···Cl distances in β-$(TeCl_3)(AlCl_4)$.

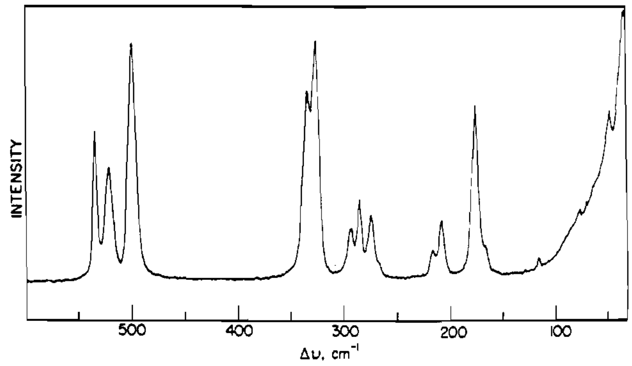

Figure 5. Raman spectrum of $(SCl_3)(SbCl_6)$.

Raman Spectra

The number of bands observed in the Raman spectrum of $(SCl_3)(SbCl_6)$ shows that the SCl_3^+ and $SbCl_6^-$ ions must be distorted from their free-ion symmetries of C_{3v} and O_h, respectively (Tables VII and VIII, Figure 5). The site symmetries of SCl_3^+ and $SbCl_6^-$ in the crystal are C_s and C_i, respectively. A complete factor group analysis is not necessary here. From the correlation diagram (Figure 6) and polarization and assignment data for $(SCl_3)(AlCl_4)$,[41] the bands at 500 and 275 cm^{-1} are respectively assigned to the nondegenerate symmetric stretch and bend of SCl_3^+. The other Raman active modes of a C_{3v} MX_3^+ ion are degenerate E vibrations. They are split here into A′ and A″

---

(40) Hartl, H.; Rama, M.; Simon, A.; Deiseroth, H.-J. *Z. Naturforsch., B: Anorg. Chem., Org. Chem.* **1979**, *34B*, 1035.

(41) Doorenbos, H. E.; Evans, J. C.; Kagel, R. O. *J. Phys. Chem.* **1970**, *74*, 3385.

Table VIII. Raman Bands (cm^{-1}) of the Cations MX_3^+ (M = S; X = Cl, Br), $SeCl_3^+$, and $TeCl_3^+$

SCl_3^+

	AsF_6^- [a]	SO_3Cl^- [b]	$AlCl_4^-$ [b,c]		$NbCl_6^-$ [d]	$TaCl_6^-$ [d]	$SbCl_6^-$ [e-g]			ICl_4^- [h]		$SnCl_6^{2-}$ [b,i]	
$\nu_1(A_1)$	519	509	494	498	496	497	500	501	500	485[j]	482[k]	484	483
$\nu_2(A_1)$	284	284	271	276	275	265	~273[l]	280	275	279	282	269	270
$\nu_3(E)$	543	526 519	530 516	533 521	519 516	532 518	532 525[l]	535 524	535 521	512 498	510 496	516	515
$\nu_4(E)$	214	228 221	206	215 208	215 210	215		210	216 208	212	205	207	207

$SeCl_3^+$

	AsF_6^- [a]	SO_3Cl^- [b]	$AlCl_4^-$ [b]	$GaCl_4^-$ [b]	$NbCl_6^-$ [d]	$TaCl_6^-$ [d]	$SbCl_6^-$ [e-g,m]			
$\nu_1(A_1)$	437	416	416	418	405	405	412	406	407	412
$\nu_2(A_1)$	200	207	...	204	195	198		197	198	203
$\nu_3(E)$	390	392	395	394	...	391	395[l]		396	
$\nu_4(E)$	168	181	186	169	160	159		184	184–130[n]	192

$TeCl_3^+$

	AsF_6^- [a,g]		SO_3Cl^- [b]	$AlCl_4^-$ [b,g]		$NbCl_6^-$ [d]	$TaCl_6^-$ [d]	$SbCl_6^-$ [e-g,m]					SbF_6^- [g]
$\nu_1(A_1)$	412	411	391	392	391	408	406	395	394	395	404[j]	402[k]	406
$\nu_2(A_1)$	170	171		168–131[n]		177–144[n]	189–145[n]		184	186–145[n]	185–154[n]	185–155[n]	173–146[n]
$\nu_3(E)$	385	379	371	367	368	390–356[n]	390–358[n]	385	381	381	391	389	388
$\nu_4(E)$	150	154		168–131[n]		177–144[n]	189–145[n]	166	169	163–145[n]	185–154[n]	185–155[n]	173–146[n]

SBr_3^+

	AsF_6^- [o]	SbF_6^- [o]	$AlCl_4^-$ [p]	$AlBr_4^-$ [p]	$SbCl_6^-$ [g,p]	
$\nu_1(A_1)$	375	379	368	347	371	370
$\nu_2(A_1)$	175	175	174	170	182–163[n]	174–166[n]
$\nu_3(E)$	429	421	401	386	411	414
	414	410.5		374	388	
$\nu_4(E)$	128	127.5	135	134	133	133
			126	124	123	122

[a] Sawodny, W.; Dehnicke, K. *Z. Anorg. Allgm. Chem.* **1967**, *349*, 169. [b] Gerding, H.; Stufkens, D. J. *Rev. Chim. Miner.* **1969**, *6*, 795. [c] Reference 41. [d] Reference 44. [e] Beattie, I. R.; Chudzynska, H. *J. Chem. Soc. A* **1967**, 984. [f] Gerding, H.; Stufkens, D. J.; Grijben, H. *Recl. Trav. Chim. Pays-Bas* **1970**, *89*, 619. [g] This work. [h] Reference 23. [i] Poulsen, F. W. *Inorg. Nucl. Chem. Lett.* **1980**, *16*, 355. Raman spectra of $GaCl_4^-$, $InCl_4^-$, $TeCl_5^-$, and $ZrCl_6^{2-}$ salts are also given. [j] Form I. [k] Form II. [l] IR data. [m] Reference 42. [n] Not readily assignable. [o] Brooks, W. V. F.; Passmore, J.; Richardson, E. K. *Can. J. Chem.* **1979**, *57*, 3230. [p] Reference 43.

components, both Raman active. The pair of peaks at 535 and 521 cm^{-1} are assigned to the asymmetric stretch while the peaks at 216 and 208 cm^{-1} are assigned to the asymmetric bend. The intense doublet band at 328 cm^{-1} is assigned to the totally symmetric breathing mode of the $SbCl_6^-$ ion. Presumably it is a doublet because of factor group splitting. The ν_2 vibration, doubly degenerate in O_h symmetry, is here split into two A_g components at 293 and 286 cm^{-1}. A third vibration normally seen in the Raman spectrum of octahedral species is the triply degenerate in-plane bend. Two of the three A_g components are seen at 175 and 169 cm^{-1}. The very weak shoulder at 266 cm^{-1} is unassigned.

Our assignments for the Raman spectra of $(SeCl_3)(SbCl_6)$ and $(TeCl_3)(SbCl_6)$ agree with those of Brockner and Demiray.[42] The Raman spectrum of $(SBr_{1.2}Cl_{1.8})(SbCl_6)$ is consistent with the presence of the SBr_3^+ and SCl_3^+ cations, and peaks at 242 and 209 cm^{-1} may be due to SCl_2Br^+ and $SClBr_2^+$ cations.[43]

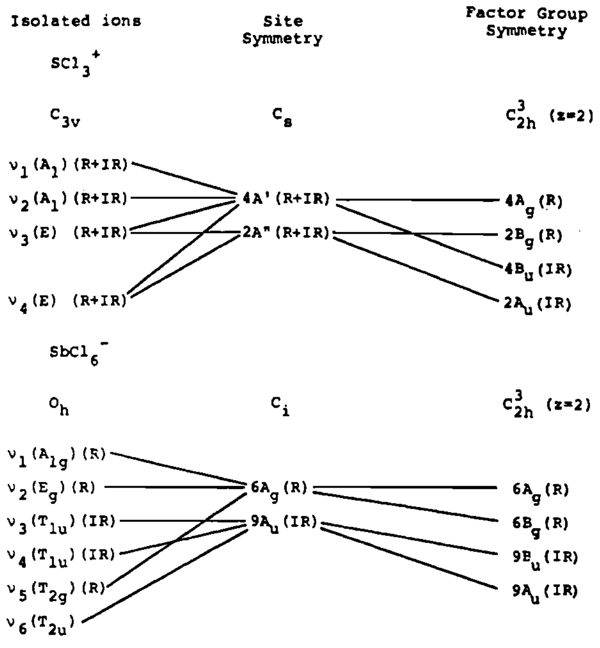

Figure 6. Correlation diagram for $(SCl_3)(SbCl_6)$.

Generally where assignments are known, the corresponding vibrations have higher frequencies for the salts than for the neutral group VB halides, consistent with the shorter M–X bonds in the cation. Three exceptions are ν_1 in $(SCl_3)(SbCl_6)$, $(SBr_{1.2}Cl_{1.8})(SbCl_6)$, and $(SeCl_3)(SbCl_6)$. An examination of the data in Table VIII shows that ν_1 and ν_2 of the MX_3^+ ions usually decrease with an increase in the Lewis basicity of the anion. This may be related to the donation of electron density from the anion to the antibonding orbitals associated with the chalcogen–halogen bonds. For example, the frequency of ν_1 for SCl_3^+ decreases from 500 to 485 cm^{-1} in the $SbCl_6^-$ and ICl_4^- salts, respectively, consistent with the observed longer S–Cl primary bond lengths in the ICl_4^- salt (cf ref 21d). Similarly, ν_1 of $TeCl_3^+$ occurs at successively higher frequencies in the Raman spectra of $TeCl_4$, $(TeCl_3)(AlCl_4)$, and $(TeCl_3)(AsF_6)$, consistent with a decrease in the primary Te–Cl bond length in the same series.[31] This stretch occurs at a higher frequency in $(TeCl_3)(SbCl_6)$ than in $(TeCl_3)(AlCl_4)$, indicating that anion–cation interactions are weaker and the Te–Cl primary bonds somewhat shorter in the $SbCl_6^-$ salt than in the $AlCl_4^-$ salt. The frequencies of ν_1 and ν_2 of $SbCl_6^-$ decrease in the series of SCl_3^+, $SeCl_3^+$, and $TeCl_3^+$ salts (Table VII), consistent with an increase in the strength of the interionic

---

(42) Brockner, W.; Demiray, A. F. *Z. Naturforsch. A: Phys., Phys. Chem., Kosmophys.* **1980**, *35A*, 766; *Z. Anorg. Allg. Chem.* **1980**, *469*, 27.

(43) Askew, H. F.; Gates, P. N. *J. Chem. Res., Synop.* **1980**, 116.

contacts in going down a group, as described above.

It has been suggested that there are no "free" $SeCl_3^+$ ions in $(SeCl_3)(NbCl_6)$ and $(SeCl_3)(TaCl_6)$ because the Se-Cl stretch occurs at 405 cm^{-1} which is considered to be too low.[44] A $Tl_2Cl_9^{2-}$ type structure or an edge-bridging model ($Cl_3SbCl_2MCl_4$, M = Nb, Ta) were favored. In $(SeCl_3)(SbCl_6)$, ν_1 is found in the Raman spectrum of 407 cm^{-1}. In addition, the similar sizes of the elements niobium, tantalum, and antimony in the +5 oxidation state (effective ionic radii 0.65, 0.65, and 0.61 Å, respectively[45]) and the existence of the dimer $SbNbCl_{10}$[46] rather than a salt like $(NbCl_4)(SbCl_6)$ all suggest a similar basicity for the three hexachloro anions. One would therefore expect $(SeCl_3)(NbCl_6)$ and $(SeCl_3)(TaCl_6)$ to contain the $SeCl_3^+$ ion. There may however be slightly stronger interionic interactions in the latter compounds.

Acknowledgment. We thank the Natural Sciences and Engineering Research Council of Canada for financial support of this work.

Registry No. $(SCl_3)(SbCl_6)$, 36487-44-2; $(SeCl_3)(SbCl_6)$, 16460-43-8; $(TeCl_3)(SbCl_6)$, 16460-42-7; $(TeCl_3)(AlCl_4)$, 36570-59-9; $(TeCl_3)(AsF_6)$, 19709-82-1; $(TeCl_3)(SbF_6)$, 99583-55-8; $(TeF_3)_2(SO_4)$, 99583-56-9; $(TeCl_3)(NbCl_6)$, 24494-45-9; As_4S_4, 12279-90-2; SbF_5, 7647-18-9; As, 7440-38-2; Se, 7782-49-2; $SeCl_4$, 10026-03-6; S, 7704-34-9; Br_2, 7726-95-6; Te, 13494-80-9; $AlCl_3$, 7446-70-0; S_7TeCl_2, 27669-14-3; AsF_5, 7784-36-3; $TeCl_4$, 10026-07-0; SO_2, 7446-09-5.

Supplementary Material Available: Tables IX-XXI containing complete bond lengths and bond angles for $(SCl_{1.2}Br_{1.8})(SbCl_6)$, $(SeCl_3)(SbCl_6)$, $(TeCl_3)(AlCl_4)$, $(TeCl_3)(AsF_6)$, $(TeCl_3)(SbF_6)$, and $(TeF_3)_2SO_4$ and anisotropic thermal parameters and final structure factor amplitudes for each compound and supplementary Figures 7-13 showing the crystal packing in $(SCl_3)(SbCl_6)$, $(SCl_{1.2}Br_{1.8})(SbCl_6)$, α- and β-$(TeCl_3)(AlCl_4)$, $(TeCl_3)(AsF_6)$, $(TeCl_3)(SbF_6)$, and $(TeF_3)_2(SO_4)$ (76 pages). Ordering information is given on any current masthead page.

---

(44) Poulsen, F. W.; Berg, R. W. *J. Inorg. Nucl. Chem.* **1978**, *40*, 471.

(45) Huheey, J. E. "Inorganic Chemistry: Principles of Structure and Reactivity"; 2nd ed., Harper and Row; New York, 1972.

(46) Bues, W.; Demiray, A. F.; Brockner, W. *Spectrochim. Acta, Part A* **1976**, *32A*, 1623.

(47) The periodic group notation in parentheses is in accord with recent actions by IUPAC and ACS nomenclature committees. A and B notation is eliminated because of wide confusion. Groups IA and IIA become groups 1 and 2. The d-transition elements comprise groups 3 through 12, and the p-block elements comprise groups 13 through 18. (Note that the former Roman number designation is preserved in the last digit of the new numbering: e.g., III → 3 and 13.)

Contribution from the Department of Chemistry, College of Arts and Sciences,
The University of Tokyo, Komaba, Megruo, Tokyo 153, Japan

Crystal Structures of (α,ω-Diaminoalkane)cadmium(II) Tetracyanonickelate(II)-Aromatic Molecule Inclusion Compounds. 3. (1,4-Diaminobutane)cadmium(II) Tetracyanonickelate(II)-Pyrrole (1/1), (1,4-Diaminobutane)cadmium(II) Tetracyanonickelate(II)-Aniline (2/3), and (1,4-Diaminobutane)cadmium(II) Tetracyanonickelate(II)-*N*,*N*-Dimethylaniline (1/1)

Shin-Ichi Nishikiori and Toschitake Iwamoto*

Received June 24, 1985

The crystal structures of three inclusion compounds of pyrrole (**1**), aniline (**2**), and *N*,*N*-dimethylaniline (**3**), each of the aromatics being accommodated respectively as the guest in the three-dimensional metal complex host structure of (1,4-diaminobutane)cadmium(II) tetracyanonickelate(II), have been determined by X-ray diffraction methods. Compound **1**, $Cd[NH_2(CH_2)_4NH_2]Ni(CN)_4\cdot C_4H_5N$, crystallizes in the monoclinic space group $P2/m$, with the lattice parameters a = 7.840 (4) Å, b = 7.634 (2) Å, c = 7.060 (2) Å, β = 90.15 (6)°, and Z = 1; the final conventional R = 0.046 has been obtained for 1488 reflections. Compound **2**, $Cd[NH_2(CH_2)_4NH_2]Ni(CN)_4\cdot 1.5C_6H_5NH_2$, crystallizes in the triclinic system $P\bar{1}$, with a = 9.774 (3) Å, b = 13.918 (8) Å, c = 7.715 (4) Å, α = 90.41 (4)°, β = 90.43 (5)°, γ = 93.18 (4)°, and Z = 2; final R = 0.066 for 2982 reflections. Compound **3**, $Cd[NH_2(CH_2)_4NH_2]Ni(CN)_4\cdot C_6H_5N(CH_3)_2$, is monoclinic, $P2_1/m$, with a = 9.860 (5) Å, b = 15.267 (6) Å, c = 7.309 (4) Å, β = 113.92 (4)°, and Z = 2; final R = 0.057 for 3126 reflections. The substantial feature of the host structure common to these three inclusion compounds is its three-dimensional framework built by the stacking of two-dimensionally extended *catena*-[cadmium(II) tetrakis(μ-cyano)nickelate(II)] sheets and the ambident bridging of 1,4-diaminobutane ligands between the adjacent cyanometal complex sheets at each cadmium atom; the cadmium atom is six-coordinated by nitrogen atoms by four N ends of the CN^- groups and two N ends of the two 1,4-diaminobutane ligands in a trans configuration. The flexibility of the host structures is observed in the manner of waving of the two-dimensional cyanometal complex sheet and in the skeletal conformation of the bridging 1,4-diaminobutane ligand, both the manner of waving and the conformation being dependent on the geometry of the guest molecule.

Introduction

The three-dimensional metal complex (α,ω-diaminoalkane)cadmium(II) tetracyanonickelate(II) accommodates several kinds of aromatic molecules as guests to give a series of inclusion compounds.[1] The series have been derived from the Hofmann-type clathrate $Cd(NH_3)_2Ni(CN)_4\cdot 2G$ (G = C_4H_4S, C_4H_5N, C_6H_6, C_6H_5OH, or $C_6H_5NH_2$).[2] In order to increase the inclusion ability of the metal complex host for substituted aromatic molecules bulkier than those designated as G in the formula, the pair of ammine ligands protruding from adjacent square-planar cadmium(II) tetracyanonickelate(II) sheets were replaced by the α,ω-diaminoalkane. The crystal structures of (1,4-diaminobutane)cadmium(II) tetracyanonickelate(II)-2,5-xylidine (1/1)[3] and (1,6-diaminohexane)cadmium(II) tetracyanonickelate(II)-*o*-toluidine (1/1)[4] were analyzed to demonstrate the inclusion structure of these compounds. As tabulated in ref 1 and 3, the guest molecules accommodated into the (diaminoalkane)cadmium(II) tetracyanonickelate(II) hosts are diverse in geometry: they range from pyrrole to 2,4,6-trimethylaniline and 1,2,3,4-tetramethylbenzene. The coefficient n of the guest molecule G in the general formula $Cd(diaminoalkane)Ni(CN)_4\cdot nG$ varies from 1 to 2, but no distinct correlation has been observed between the

---

(1) Hasegawa, T. Nishikiori, S.; Iwamoto, T. *J. Inclusion Phenom.* **1983**, *1*, 365.

(2) Iwamoto, T. In "Inclusion Compounds"; Atwood, J. L., Davies, J. E. D., MacNicol, D. D., Eds.; Academic Press: London, 1984; Vol. 1, pp 29-57.

(3) Nishikiori, S.; Iwamoto, T. *J. Inclusion Phenom.* **1985**, *2*, 341.

(4) Hasegawa, T.; Nishikiori, S.; Iwamoto, T. *J. Inclusion Phenom.* **1984**, *2*, 351.